

¹ **High-resolution regional climate model evaluation using variable-resolution**

² **CESM over California**

³ Xingying Huang, * Alan M. Rhoades and Paul A. Ullrich

⁴ *Department of Land, Air and Water Resources, University of California, Davis*

⁵ Colin M. Zarzycki

⁶ *National Center for Atmospheric Research*

⁷ *Corresponding author address: Xingying Huang, Department of Land, Air and Water Resources,

⁸ University of California Davis, Davis, CA 95616.

⁹ E-mail: xyhuang@ucdavis.edu

ABSTRACT

10 Understanding the effect of climate change at regional scales remains a
11 topic with intensive researches. Due to computational constraints, high hor-
12 izontal resolutions required to reach regional scales have been largely out of
13 reach for current global climate models. However, high resolution is needed
14 to represent fine-scale processes and topographic forcing, which is a signif-
15 icant driver of local climate variability. Although regional climate models
16 (RCMs) have been widely used at these scales, variable-resolution global cli-
17 mate models (VRGCMs) have arisen as an alternative for studying regional
18 weather and climate. In this paper, the recently developed variable-resolution
19 option within the Community Earth System Model (CESM) is assessed for
20 long-term regional climate modeling. The mean climatology of temperature
21 and precipitation, across California's diverse climate zones, is analyzed and
22 contrasted with the Weather Research and Forcasting (WRF) model (as a tra-
23 ditional RCM), regional reanalysis, gridded observational datasets and a uni-
24 form high-resolution CESM with the finite volume (FV) dynamical core. The
25 results show that variable-resolution CESM is competitive in representing re-
26 gional climatology on both annual and seasonal time scales. This assessment
27 adds value to the use of VRGCMs for projecting climate change over the
28 coming century and improve our understanding of both past and future re-
29 gional climate related to fine-scale processes. This assessment is also relevant
30 for addressing the scale limitation of current RCMs or VRGCMs when next-
31 generation model resolution increases to $\sim 10\text{km}$ and beyond.

³² **1. Introduction**

³³ Global climate models (GCMs) have been widely used to simulate both past and future cli-
³⁴ mate. Although GCMs have demonstrated the capability to successfully represent large-scale
³⁵ features of the climate system, they are usually employed at coarse resolutions ($\sim 1^\circ$), largely
³⁶ due to computational limitations. Global climate reanalysis datasets, which assimilate climate
³⁷ observations using a global model, represent a best estimate of historical weather patterns, but
³⁸ still have relatively low resolutions no finer than 0.5° (<http://reanalyses.org/atmosphere/>
³⁹) overview-current-reanalyses). Consequently, regional climate is not well captured by either
⁴⁰ GCMs or global reanalysis datasets. However, dynamical processes at unrepresented scales are
⁴¹ significant drivers for regional and local climate variability, especially over complex terrain (?). In
⁴² order to capture these fine-scale dynamical features, high horizontal resolution is needed to allow
⁴³ for a more accurate representation of fine-scale forcings, processes and interactions (??). With
⁴⁴ these enhancements, the regional climate information is expected to be more usable for policy
⁴⁵ makers and local stakeholders in formulating climate adaptation and mitigation strategies.

⁴⁶ In order to model regional climate at high spatial and temporal resolution over a limited area,
⁴⁷ downscaling methods have been developed. There are largely two approaches for downscaling
⁴⁸ including statistical downscaling and dynamical downscaling. Dynamical downscaling is popu-
⁴⁹ lar and commonly employed using nested limited-area models (LAMs) or by applying a variable
⁵⁰ resolution GCM (VRGCM) to model regional scales (?). In this context, LAMs are typically re-
⁵¹ ferred as regional climate models (RCMs) when applied to climate scales. Forced by output of
⁵² GCMs or reanalysis data, RCMs have been widely used, particularly to capture physically con-
⁵³ sistent regional and local circulations at the needed spatial and temporal scales (????). Recently,
⁵⁴ VRGCMs have been increasingly employed for modeling regional climate. This approach uses

55 a global model that includes high-resolution over a specific region and coarse resolution over the
56 remainder of the globe (??). And there are different strategies to achieve high-resolution over the
57 area of interest such as stretched-grid models or grid refinement technique (???). VRGCMs have
58 been demonstrated to be effective for regional climate studies and applications at a reduced com-
59 putational cost compared to uniform GCMs (????). Fox et al. (2000) found that the stretched-grid
60 version of a GCM captured not only large-scale meteorological patterns as traditional GCMs did
61 but also mesoscale features especially when considering orographic forcing (?).

62 Compared with RCMs, a key advantage of VRGCMs is that they use a single, unified modeling
63 framework, rather than a separate GCM and RCM. Thus, VRGCMs avoid potential inconsistency
64 between the global and regional domains, and naturally support two-way interaction between these
65 domains without the need for nudging (????). However, in order to obtain deeper insight into the
66 performance of these two modeling approaches, it is necessary to compare them directly. For the
67 purposes of this paper, we will focus on the recently developed variable-resolution Community
68 Earth System Model (varres-CESM) using the grid refinement technique as our VRGCM of inter-
69 est. Although CESM has been well-used for uniform resolution modeling, variable-resolution in
70 the Community Atmosphere Models (CAM) Spectral Element (SE) dynamical core has only been
71 recently developed. ? applied this option in CAM-SE and showed that high-resolution simulation
72 of topical cyclones represented significant improvements over the unrefined simulation. Zarzycki
73 et al. also compared the large-scale features of varres-CESM 0.25° and uniform CESM at one
74 degree, and found that adding refined region over the globe did not affect the global circulation
75 noticeably (??).

76 However, varres-CESM has yet to be rigorously investigated for long-term regional climate sim-
77 ulation (??). And in this paper, it is the first time to investigate whether VRGCMs can show similar
78 or even better ability in regional climate modeling compared with traditional method of RCMs.

79 The goal of this paper is to evaluate the performance of varres-CESM against gridded observational
80 data, reanalysis data and in comparison to a RCM. Also, outputs from a uniform high-resolution
81 CESM simulation have also been utilized here (?). Our variable-resolution simulations will focus
82 on relatively high resolutions for climate assessment, namely 28km and 14km grid spacing, which
83 are much more typical for dynamically downscaled studies. For comparison with the more widely
84 used RCM method, the Weather Research and Forecasting (WRF) model will be applied at 27km
85 and 9km grid spacing (?). The study focuses on models' ability to represent current climate statis-
86 tics, particularly those relative to climate extremes. We anticipate that this assessment will add
87 value in modeling mean regional climatology and improve our understanding about the effects of
88 multi-scale processes in regional climate regulation. Our goal is also to advance the understanding
89 of better use of models in future climate predictions and climatic extremes studies regionally.

90 In this paper, we use California (CA) as our study area. With its complex topography, coastal
91 influences, and wide latitudinal range, this makes CA an excellent test bed. Also, an understanding
92 of local climate variability is incredibly important for policymakers and stakeholders in California
93 due to its vast agricultural industry, wide demographics, and vulnerability to anthropogenically-
94 induced climate change (??). RCM simulations over California have also been conducted in pre-
95 vious studies and showed the need of high resolution to better study regional climate and extreme
96 events, especially over complex topography with large climate gradients (?????). ?, in particular,
97 presented results from WRF (Weather Research and Forecasting) at 12km spatial resolution show-
98 ing both the overall consistency and some biases (e.g. overestimation of precipitation) between
99 simulations and observations.

100 This paper is organized as follows. Section 2 describes the model setup, verification data and
101 evaluation methods. In section 3, results are demonstrated focusing on 2 m temperature (Ts) and
102 precipitation (Pr). Key results are summarized along with further discussion in section 4.

103 **2. Models and Methodology**

104 *a. Simulation design*

105 All simulations use the AMIP (Atmospheric Model Intercomparison Project) protocols (?).
106 AMIP simulations attempt to recreate a climatology similar to that observed over the past few
107 decades, with prescribed sea-surface temperatures (SSTs) and ice concentrations.

108 1) VARRES-CESM

109 CESM is a state-of-the-art Earth modeling framework developed by the National Center for
110 Atmospheric Research (NCAR), consisting of atmospheric, oceanic, land and sea ice components
111 and has been heavily used for understanding the effects of global climate change (??). Different
112 component models are connected by a couple component. In this way, the interfacial states and
113 fluxes between the various component models are communicated and the fluxed quantities are
114 conserved. Since we follow AMIP protocols in this study, communication is mainly occurred
115 between atmospheric and land model. Ocean model and sea ice component are disabled. Here,
116 CAM version 5 (CAM5) (?) and the Community Land Model (CLM) version 4 (?) are used. As
117 mentioned earlier, SE was used as the dynamical core in CAM along with the variable-resolution
118 grid support. The FAMIP5 (F_AMIP_CAM5) compset was chosen for the simulations as it is the
119 standard protocol for AMIP and is less computationally demanding.

120 For our study, the variable-resolution cubed-sphere grids are generated for use in CAM and
121 CLM with the open-source software package SQuadGen (?). The grids used are depicted in Fig-
122 ure ???. The maximum horizontal resolution on these grids are 0.25 degree ($\sim 28\text{km}$) and 0.125
123 degree ($\sim 14\text{km}$) respectively, with one degree resolution covering the rest of the globe. These
124 resolutions have been selected because CAM-SE naturally supports a 2:1 aspect ratio, meaning

125 there are two transition layers from 1 degree to 0.25 degree, and one additional transition from
126 0.25 degree to 0.125 degree. The meteorological patterns (e.g. wind, pressure and precipitation)
127 showed natural and conserved results over the transition boundary as described in (?). The time
128 period is from 1979-01-01 to 2005-12-31 (UTC), and year 1979 was discarded as spin up time for
129 CLM4.0. We chose this time period to present the recent historical climate and try to achieve the
130 best balance between reproducibility and computational feasibility, which is further discussed in
131 the Methodology part.

132 Variable-resolution topography files have been produced by starting with the National Geophys-
133 ical Data Center (NGDC) 2-min (\sim 3.5 km) Gridded Global Relief Dataset (ETOPO2v2) topog-
134 raphy dataset and applying the differential smoothing technique by adjusting the c parameter from
135 Eq. (1) in ?. The grid-scale topography is showed in Figure ???. The higher resolution simulations
136 provide a much finer representation of regional topography. This is important for understanding
137 local climate since topography is an important driver for fine-scale dynamic processes, especially
138 over complex terrain.

139 Land surface datasets, and plant functional types, were created at the standard 0.50 degree res-
140 olution. Initialized conditions are provided for both CAM and CLM. Greenhouse gas (GHG)
141 concentrations are prescribed based on historical observations. SSTs and ice coverage are sup-
142 plied by the one degree Hadley Centre Sea Ice and Sea Surface Temperature dataset (HadISST)
143 (?). Tuning parameters are not modified from their default configuration.

144 2) UNIFORM CESM

145 Output from a globally uniform CESM run at 0.25° spatial resolution is utilized for compari-
146 son. It helps us to see if variable-resolution CESM, which is at much lower computation cost than
147 uniform one, can show comparable performance in modeling mean climatology (?). This globally

¹⁴⁸ uniform simulation uses the CAM5-FV (finite volume) dynamical core and is described in addi-
¹⁴⁹ tional detail in ? and ?. need to add details about this and which parameters are different from the
¹⁵⁰ public version.

¹⁵¹ 3) WRF

¹⁵² WRF has gained wide acceptance in studying regional climate over the past decade, showing
¹⁵³ its adequate capability in representation of fine-scale climate properties (???). In this study, the
¹⁵⁴ fully compressible non-hydrostatic WRF model in version 3.5.1 with the Advanced Research WRF
¹⁵⁵ (ARW) dynamical solver is used. ERA (ECMWF re-analysis)-Interim data at surface and pressure-
¹⁵⁶ level was used to provide initial and lateral conditions for the domains. The lateral conditions and
¹⁵⁷ SSTs were updated every 6 hours. ERA-Interim reanalysis (~ 80 km) has been widely used and
¹⁵⁸ validated for its reliability as forcing data (?). Two simulations are conducted with finest horizontal
¹⁵⁹ resolution of 27km and 9km respectively, over the same time period as varres-CESM. The ~ 10
¹⁶⁰ km resolution is actually finer than most previous studies for long-term climate. Also, the year
¹⁶¹ 1979 is used as a spin-up period and is discarded for purposes of analysis.

¹⁶² The simulation domains of WRF are depicted in Figure ???. For the WRF 27km simulation, one
¹⁶³ domain is used. For the WRF 9km simulation, two nested domains are used with the outer domain
¹⁶⁴ at 27km (same as the WRF 27km) and inner domain at 9km horizontal grid resolution, satisfying
¹⁶⁵ the natural WRF refinement ratio of 3:1. As a common way in WRF, two-way nesting is enabled by
¹⁶⁶ feeding back information from the fine grid onto the coarse grid, thus the nested region's process
¹⁶⁷ of the coarse domain is replaced by the fine grid result (?). Both grids are centered on CA and have
¹⁶⁸ respectively, 120×110 and 151×172 grid points. Around the boundaries, 10 grid points are used as
¹⁶⁹ lateral relaxation zones. In order to reduce the drift between forcing data and RCM, grid nudging
¹⁷⁰ (?) was applied to the outer domain every 6 hours at all levels except the planetary boundary

¹⁷¹ layer (PBL) as suggested by ?. This setup uses 41 vertical levels with model top pressure at 50
¹⁷² hPa. The topography data used in 27km and 9km are interpolated from USGS (U.S. Geological
¹⁷³ Survey) elevation data with 10m and 2m resolution respectively. The grid-scale topography is
¹⁷⁴ contrasted in Figure ???. Some differences are also apparent between the 28km varres-CESM and
¹⁷⁵ 27km WRF model, particularly over the Central Valley, and indicative of a different methodology
¹⁷⁶ for preparation of the topography dataset.

¹⁷⁷ Additionally, we used the following physics parameterizations: WSM (WRF Single-Moment)
¹⁷⁸ 6-class graupel microphysics scheme (?), Kain-Fritsch cumulus scheme (?), CAM shortwave and
¹⁷⁹ longwave radiation schemes (?). These settings are supported by the one-year test running result
¹⁸⁰ with different options of cumulus scheme and radiation schemes. For the boundary layer, the
¹⁸¹ Yonsei University scheme (YSU) (?) and the Noah Land Surface Model (?) were used. Both
¹⁸² were chosen as they are common for climate applications that balance long-term reliability and
¹⁸³ computational cost.

¹⁸⁴ *b. Datasets*

¹⁸⁵ For validation purpose, available reanalysis and gridded observational datasets of the highest
¹⁸⁶ quality are employed (see Table ??). Although gridded observational datasets are generally based
¹⁸⁷ on measurements of weather stations, they are based on different network of stations. And these
¹⁸⁸ datasets are scaled and gridded using varied interpolation techniques, elevation models and pro-
¹⁸⁹ cessing algorithms. In this way, using multiple reference datasets rather than one is important
¹⁹⁰ to account for the uncertainties, when assessing the performance of the WRF and CESM simu-
¹⁹¹ lations in terms of both mean behavior and variability. Moreover, in this study, our purpose of
¹⁹² using these products is to serve as realistic proxies to allow for a comparison of the model results.
¹⁹³ We acknowledge that reanalysis products are particularly sensitive to model choice and choice of

¹⁹⁴ assimilated observations and so cannot be treated as truth. Detailed descriptions of these datasets
¹⁹⁵ are as follows.

¹⁹⁶ (i) *NARR*: The North American Regional Reanalysis (NARR) provides dynamically downscaled
¹⁹⁷ data over North America at ~ 32 km resolution and 3 hourly intervals from 1979 through present
¹⁹⁸ (?). It is National Centers for Environmental Prediction (NCEP)'s high resolution reanalysis prod-
¹⁹⁹ uct. All major climatological variables are present in NARR, making it an excellent candidate for
²⁰⁰ assessment of regional climate. Nonetheless, some inaccuracies have been identified in NARR
²⁰¹ that must be accounted for, including deficiencies in precipitation fields away from the continental
²⁰² US (?).

²⁰³ (ii) *NCEP CPC*: This data set is CPC unified gauge-based analysis of daily precipitation pro-
²⁰⁴ vided by the National Oceanic and Atmospheric Administration (NOAA) Climate Prediction Cen-
²⁰⁵ ter (CPC). It is a suite of unified precipitation products with consistent and improved quality by
²⁰⁶ combining all information available at CPC and by taking advantage of the optimal interpolation
²⁰⁷ (OI) objective analysis technique. The gauge analysis covers the Conterminous United States with
²⁰⁸ a fine-resolution at 0.25° from 1948/01/01 to 2006/12/3.

²⁰⁹ (iii) *UW*: The UW daily gridded meteorological data is obtained from the Surface Water Mod-
²¹⁰ eling group at the University of Washington (??). UW incorporated topographic corrections by
²¹¹ forcing the long-term average precipitation to match that of the PRISM dataset. Temperature
²¹² dataset is produced in a similar fashion as precipitation, but used a simple 6.1 K/km lapse rate for
²¹³ topographic effect. The dataset is at 0.125° horizontal resolution and provided from year 1949 to
²¹⁴ 2010.

²¹⁵ (iv) *PRISM*: The Parameter-elevation Regressions on Independent Slopes Model (PRISM) (?)
²¹⁶ supports a 4km gridded dataset obtained by taking wide range of point measurements and apply-

²¹⁷ ing a weighted regression scheme that accounts for many factors affecting the local climatology.
²¹⁸ The datasets include total precipitation and minimum/maximum, (derived) mean temperatures and
²¹⁹ dewpoints, based on sophisticated quality control measures. Monthly climatological variables are
²²⁰ available for 1895 through 2014 provided by the PRISM Climate Group. PRISM is U.S. Depart-
²²¹ ment of Agriculture (USDA)'s official climatological data. We will use this product as the main
²²² reference dataset for model assessment.

²²³ (v) *Daymet*: Daymet is an extremely high resolution (1 km) gridded dataset with daily outputs
²²⁴ of total precipitation, humidity, and minimum/maximum temperature covering the years of 1980
²²⁵ through 2013 (???). The dataset is produced using an algorithmic technique that ingests point
²²⁶ station measurements in conjunction with a truncated Gaussian weighting filter. Some adjust-
²²⁷ ments are made to account for topography. Daymet is available through the Oak Ridge National
²²⁸ Laboratory Distributed Active Archive Center (ORNL DAAC).

²²⁹ c. *Methodology*

²³⁰ Near surface (2 meter) temperature and precipitation have been analyzed over California, to
²³¹ assessing the models' performances in representing the mean climatology. Specifically, evaluation
²³² focuses on daily maximum, minimum and average 2m temperatures (Tmax, Tmin and Tavg), and
²³³ daily precipitation (Pr). These variables are key for a baseline climate assessment, particularly
²³⁴ for their relationship with water resources, agriculture and health. With the overall warm climate
²³⁵ and large impact of heat waves over CA, we focus on the summer season covering June, July and
²³⁶ August (JJA) in the aspect of temperature. Since the vast majority of precipitation in CA occurs
²³⁷ in the winter season, together with the accumulation of snowpack, in this way, precipitation over
²³⁸ December-January-February (DJF) is emphasized.

239 In order to adequately account for natural variability even at regional scale, simulations need to
240 be run long enough (?). However, there is no particular timeframe for climatology studies. Aver-
241 age weather conditions over 30-year or so are typically used to track climate to make sure that the
242 data is long enough to calculate an average that is not influenced by year-to-year variability (?). In
243 this study, 26-year current-climate runtime is chosen to reasonably balance the reproducibility and
244 computational availability. We have studied the variability of mean temperature and precipitation
245 in both simulations and observations over 5, 10, 20 and 25 seasons or years, and the results showed
246 that 20 or 25 years' simulation are long enough to adequately capture the regionally climate vari-
247 ability. 30 years or longer run time may sound better, but are not necessary for our case.

248 All the results showed in the following part are based on the time period from year 1980 to 2005.
249 All the datasets have been investigated first to see if time trend exists over this 26 years period, and
250 the least squares linear trend has been removed from original datasets if existing. It is found that
251 for temperature, there do have statistically significant linear trend over some parts of CA under the
252 two-tailed t-statistic significance level of 0.05. However, no significant trend has been detected for
253 precipitation.

254 Further, in order to better assess the treatment of California's varied climate regions, the state
255 has been divided into five regional zones, including: the Central Valley, Mountain Region, North
256 Coast, South Coast, and Desert Region as showed in Figure ???. The division of these five zones
257 are loosely based on the results of ? and the building climates zones from California Energy Com-
258 mission. For parts of the results analyses, simulations and datasets are masked to restrict climate
259 variables to specific zones. We aim to examine the statistics of data averaged over geographic
260 climate zones instead of just on grid-cell analysis.

261 Statistical measurements have been used to quantify the performances of the models comparing
262 with the reference datasets. These statistical variables include the Root-mean-square deviation

263 (RMSD), mean absolute difference (MAD), mean relative difference (MRD) and correlation, and
264 sample standard deviation.

265 When calculating the difference at grid point, the reference datasets are remapped to the given
266 model's output resolution. Datasets are remapped using a bilinear interpolation method, which
267 has been verified to provide satisfactory performance. Other remapping algorithms, such as patch-
268 based have been tested and do not exhibit notable differences.

269 Student's t-test is used when necessary to see if two sets of yearly or seasonally averaged data are
270 significantly different from each other, and 0.05 is used as critical levels of significance. We need
271 to point out that this is just a approximate test to further support our results analysis since the two
272 populations being compared should follow a normal distribution.

273 3. Results

274 a. Temperature

275 The mean JJA Tmax, Tmin and Tavg climatology over 26 years of simulations together with
276 PRISM are shown in Figure ??. The statistical measurements over whole CA area are showed
277 in Table ??. We can see that all simulations have captured the spatial climate patterns showed
278 by the PRISM, with high spatial correlations (>0.95), especially for Tmax and Tavg. For Tmax,
279 comparing with reference datasets, varres-CESM showed a warmer climate generally with about
280 2 to 3°C difference. Uniform CESM is similar as varres-CESM, but with a larger RMSD value
281 ($\sim 4^{\circ}\text{C}$). However, WRF output displayed overall colder climate, especially the WRF 9km, with
282 about 2 to 3°C difference. Tmax over Central Valley has been overestimated by all the simulations
283 and the possible reason has been discussed at the end of this part.

284 For Tmin, varres-CESM still showed a warm effect (~ 3 to 4°C), with a particularly egregious
285 overestimation over Nevada. WRF also had overall warm effect but displayed better performance
286 than varres-CESM with smaller differences (~ 2 to 3°C), comparing with reference datasets. How-
287 ever, the pattern of Tmin presented in Figure ?? in both WRF simulations suggests a cooler interior
288 to the Central Valley and warmer perimeter, which is not supported by observations. Overestima-
289 tion of Tmin and Tmax by varres-CESM leads a similar overestimation for Tavg, so does uniform
290 CESM. And underestimation of Tmax by WRF, causes a underestimation for Tavg, but still statis-
291 tically more close to reference datasets than CESMs. The sample standard deviations of the JJA
292 Tmax, Tmin and Tavg by models and PRISM are showed in Figure ???. It can be seen that the
293 variability has little changes across difference sub-zones, and the values are around 0.5 to 1.5°C
294 for all the datasets, except some higher values ($\sim 2^{\circ}\text{C}$) over mountains regions in WRF 9km.

295 There are some minor uncertainties, as we already discussed, showed when comparing with
296 different reference datasets. We have made the Student's t-test to see if the JJA Tmax, Tmin and
297 Tavg from PRISM, UW and Daymet are statistically different from each other. And the results
298 showed that they are the same at the significance level of 0.05 over most regions of our study
299 area, except coastal regions. These observations are still of the highest quality available and the
300 uncertainty is relatively small compared with difference from the simulations, thus are unlikely
301 impacting the evaluation results.

302 Overall, varres-CESM 0.125 degree performed best in simulating long-term Tmax, and WRF is
303 better at modeling Tmin than varres-CESM. When comparing against NARR (not showed), the
304 overestimation of Tmin are largely reduced for varres-CESM. This suggests that the source of the
305 temperature bias in varres-CESM and NARR may be related. Additionally, there are a positive
306 2 K SST bias near the California coastline between varres-CESM and WRF runs. This may also
307 cause overestimation of temperatures. The sea breeze effect, associated with cooler temperatures

308 near the San Francisco Bay, are apparent in all runs. It is especially encouraging that differences in
309 the varres-CESM simulations, which only used prescribed SSTs, closely matched those of WRF,
310 which were forced at the lateral domain boundaries with reanalysis data.

311 The seasonal cycle of Tavg is shown in Figure ?? for simulations and reference data from PRISM
312 and NARR. The models do show good consistency with reference data with no larger than 2°C
313 difference, which mainly occurred in the coldest and hottest seasons. Compared with PRISM,
314 Varres-CESM showed positive difference over the summer season in all sub-zones except coastal
315 regions, and negative difference over winter season in all zones, indicating larger temperature
316 range. The uniform CESM is similar to varres-CESM, with about 1°C larger difference. WRF
317 has better performance in presenting the monthly trend than CESM with about 1°C underestima-
318 tion over all seasons. No notable differences can be discerned when comparing models across
319 resolutions.

320 The variability over each month is expressed by the sample standard deviation showed in Figure
321 ???. Generally, local variability of Tavg is under 3°C , mostly within the range from 1 to 2°C .
322 Among the simulations, WRF 27km is most consistent with PRISM. WRF 9km is also close
323 to PRISM, but has $\sim 1^{\circ}\text{C}$ larger variability over January and February. Varres-CESM basically
324 showed about 0.5°C more scattered values (either above or lower) comparing to reference datasets,
325 and uniform CESM has about 0.5°C lower variability than PRISM.

326 For the temperature climatology in California, we are most interested in the Tmax over summer
327 season due to the impact of summer heat waves. We depict the frequency distribution of Tmax
328 using all the JJA daily values over 26 years. The results of the simulations and reference datasets
329 of Daymet and UW are showed in Figure ???. Properties of the frequency distribution, including
330 average, variability, skewness and Kurtosis are tabulated in Table ???. Though with some devia-
331 tions, similar distribution shapes with tails off to left are present for both models and observations.

332 Contrasting with WRF, varres-CESMs are more close to reference datasets. WRF 9km tended to
333 be colder. Models including varres-CESM and WRF 27km are more consistent with observations
334 for higher values than the peak and less consistent at lower values. For representation of heat
335 extremes, both varres-CESM and WRF 27km exhibit satisfactory performance over most regions
336 except in Central Valley (CV). No obvious improvement is associated with higher resolution in
337 varres-CESM.

338 In the Central Valley, models show a clear warm effect and associated long tail, with tempera-
339 tures reaching near 50°C. As discussed before, all models do overestimate Tmax over CV. In order
340 to further assess the accuracy of the gridded observations, we examine the Tmax data directly from
341 recorded weather station observations over the CV. The results validate that Tmax values above
342 45°C are rare (although station observations suggest these days may be slightly more frequent than
343 suggested by UW and Daymet). The warm bias associated with the aforementioned extreme hot
344 days in both varres-CESM and WRF is likely correlated with overly dry summertime soil mois-
345 ture, as discussed in ?. This could be caused by the lack of accurate land surface treatment in
346 climate models. areas. Bonfils and Lobell (2007) found that irrigation in Central Valley has sig-
347 nificantly decreased summertime maximum temperatures especially in heavily-irrigated areas (?).
348 Other studies have also found the cooling effects of irrigation, such as (?).

349 *b. Precipitation*

350 California is known for the shortage of natural water resources with extreme drought over sum-
351 mer season. In this way, the winter season is particularly important for California as it accounts
352 for 50 percent of the ~22.5 inches that California receives for its total annual average precipitation
353 amounts (<http://www.ncdc.noaa.gov/cag/>).

354 The long-term average climatologies of DJF and annual daily precipitation (Pr) over 26 years
355 from simulations and reference datasets are displayed in Figure ???. And the statistical measure-
356 ments over whole CA area are showed in Table ???. As we can see, precipitation is distributed
357 mostly along the North coast and Sierra Nevada mountains, and is relatively sparse in other re-
358 gions. As temperature, simulations also captured the spatial patterns of the PRISM, with high
359 correlation coefficients (>0.94). However, there do exist clear differences among simulations.

360 Varres-CESM overestimated precipitation, especially in the coarser resolution (28 km) simu-
361 lation (about 40%-50%) along the western side of Sierra Nevada, resulting statistical difference
362 over this area comparing with PRISM. Interestingly, varres-CESM 0.125° is statistically the same
363 as PRISM. Uniform CESM has slightly better results than varres-CESM 0.25deg . There are no-
364 table differences between WRF 27km and WRF 9km. WRF 27km underestimates precipitation
365 for about 30%, whereas WRF 9km shows a large positive difference (about 60%-80%) along the
366 North coast and the Sierra Nevada. However, considering the variability showed in the Figure
367 ???, WRF 9km and WRF 27km are both significantly the same at the significance level of 0.05 as
368 PRISM except over the mountain region. From the sample standard deviation of the precipitation
369 displayed in Figure ??, we can see that the variability has similar patterns of the precipitation
370 intensity distribution, and increases as the precipitation magnitude increases. Models seem to
371 capture the variation of precipitation well, particularly looking at the varres-CESM 0.125deg and
372 WRF 27 km, though variability is $\sim 50\%$ higher for WRF9km.

373 IThe reference datasets again showed differences indicating uncertainty inherent in interpolating
374 station data to a grid. We have also made the Student's t-test to test the if the mean precipitation
375 climatology from PRISM, UW and Daymet are statistically different from each other. And it
376 turned out that they are almost the same at the significance level of 0.05 over all the study area.
377 Therefore, the uncertainties within them are negligible. Overall, varres-CESM 0.125° performs

378 slightly better than CESM 0.25° and WRF 27km, as further exhibited by the RMSD values in
379 Table ??.

380 The annual cycle of precipitation averaged over each sub-zone over 26 years is presented in
381 Figure ???. It can be seen that simulations showed similar trend as reference datasets. The main
382 deviation occurred during the rainy seasons, especially in winter. WRF 27km is drier and WRF
383 9km is far wetter in all regions as discussed above. Varres-CESM tracks well with observed pre-
384 cipitation everywhere except in the Central Valley, where precipitation is overestimated at rainy
385 seasons with about 70%-80%. Nonetheless, the strong seasonal dependence on precipitation is
386 apparent with extremely dry conditions during summer months. A slight increase in summertime
387 precipitation is apparent in the Desert region, indicating the North American monsoon. Over-
388 all, varres-CESM is more consistent with observations compared with WRF. However, we also
389 observe that the peak month for precipitation tends to occur earlier in varres-CESM than in obser-
390 vations. It is not surprising that a seasonal time drift occurred with the varres-CESM simulations
391 as it was not forced by a reanalysis dataset (unlike the WRF simulations).

392 The variability over each month is expressed by the sample standard deviation showed in Figure
393 ???. The variability has similar monthly trend as the annual cycle of precipitation, with overall
394 value from 0 to 4 mm/day, which generally shows higher inter-annual variability over locations
395 of higher mean precipitation ???. Comparing with observations, varres-CESM exhibited a slightly
396 larger variability (basically no more than 1mm/day) in the rainy season, while WRF 27km has
397 better representation with a little lower values. WRF 9km again showed larger variability (about
398 \sim 1mm/day more) during rainy seasons over most regions. Such higher variability within higher
399 magnitude of precipitation has also been found in previous studies. Duffy et al. (2006) discussed
400 the higher variability caused by higher spatial resolution used in RCM models, with more accurate
401 representation of topography (?). The main cause of the interannual variability of precipitation

402 over CA is El NioSouthern Oscillation (ENSO), which varies the amount of moisture flux trans-
403 ported to this region.

404 The frequency distribution of DJF Pr has been constructed from rainy days in winter
405 ($\text{Pr} \geq 0.1 \text{ mm/d}$) and depicted in Figure ???. Within our expectation, it can be seen that varres-
406 CESM is more consistent with observations everywhere except in the CV. In this region WRF
407 27km appears to better capture high-intensity precipitation events, but performs more poorly on
408 low-intensity events. The underestimation of rainfall frequency in WRF 27km appears consis-
409 tent across regions. WRF 9km produces a significantly better treatment of low-intensity events,
410 but greatly overestimates the frequency of high-intensity events. Notably, varres-CESM 0.25 de-
411 gree and varres-CESM 0.125 degree do not show significant differences. For strong precipitation
412 events, varres-CESM and WRF 27km show good performance over most regions except in those
413 noted above, although these conclusions are also constrained by observational uncertainty.

414 The overestimation of precipitation for WRF at high resolution has also been found in previous
415 studies. ? showed that WRF at 12km largely overestimate the precipitation over the mountain
416 division of CA. The deviation magnitude is less than what showed in this study due to different
417 division area and perhaps different setting of physical schemes. In aforementioned Caldwell's
418 paper, possible reasons have been discussed in detail, stating a variety of source including the
419 model itself and the choice of physical parameterizations. A comprehensive analysis of the cause
420 of these errors is beyond the scope of this paper. Further discussion can be found in former
421 studies including the use of different microphysics schemes and resulting change of precipitation
422 magnitude (?????).

423 Finally, a concise summary of model performance over CA is provided by the Taylor diagram
424 (Figure ??). This diagram includes the spatial centered correlation between the simulated and
425 observed fields, the RMS variability of simulations normalized by that in the observations, and

⁴²⁶ mean differences from reference data. It can be seen that the models correlate well with the PRISM
⁴²⁷ reference dataset. Normalized standard deviation and bias are larger for precipitation, especially
⁴²⁸ for WRF 9km. Overall, varres-CESM has demonstrated that it can competitively compare to WRF
⁴²⁹ in capturing the regional climatology of California. ([update the plot](#))

⁴³⁰ 4. Discussions and summary

⁴³¹ With the need of high resolution to better study regional climate and extreme events, this study
⁴³² got deep into the use of a variable-resolution GCM (i.e. varres-CESM) as an alternative way in
⁴³³ dynamical regional climate modeling. The performance of varres-CESM has been investigated in
⁴³⁴ simulating California climatology as regional climate studies. This relatively new technique has
⁴³⁵ been evaluated against a traditional RCM (i.e. WRF) directly for the first time.

⁴³⁶ Based on 26 years of high-resolution historical climate simulations, we analyzed the mean cli-
⁴³⁷ matology of California and across its climate divisions from both temperature and precipitation,
⁴³⁸ mainly based on the output of varres-CESM and WRF. Generally, when compared with gridded
⁴³⁹ observational datasets, all simulations do a good job of capturing regional climatological patterns
⁴⁴⁰ with high spatial correlations (>0.94). Uncertainty between reference datasets exists, but is rela-
⁴⁴¹ tively small and not statistically significant over most regions. We found that varres-CESM showed
⁴⁴² comparable performance as WRF in regional climate study. Even compared with a uniform high-
⁴⁴³ resolution GCM (CESM-FV), varres-CESM also performed competitively.

⁴⁴⁴ Deviations from reference datasets do exist in these simulations, but they have different features.
⁴⁴⁵ During summer, varres-CESM model possessed about 2 to 3°C warmer climate, especially in
⁴⁴⁶ the Central Valley. WRF exhibited a colder ($\sim 2^{\circ}\text{C}$) Tmax over most regions except the Central
⁴⁴⁷ Valley, but a little warmer in Tmin. Overall, varres-CESM showed better ability in reproducing
⁴⁴⁸ mean climatology of Tmax, but WRF was better at modeling Tmin and Tavg. The variability of

449 JJA mean temperature is basically within the range of 0.5 to 1.5°C. WRF presents the annual
450 cycle of Tavg better than CESM with about 1°C underestimation. CESMs showed about 2°C
451 overestimation of Tavg over the summer season and similar magnitude of underestimation over
452 winter season, indicating larger temperature range over most regions.

453 For representation of heat extremes, both varres-CESM and WRF 27km exhibit close frequency
454 to observations over all study area except in Central Valley (CV). This is likely caused by the
455 lack of irrigation cooling effect over this region since irrigation is rarely considered in long-term
456 climate modeling. In future work, we will add irrigation effect in varres-CESM to figure out the
457 role irrigation played in regulating Tmax, and the overestimation and longer upbounded tail of
458 frequency distribution for Tmax,

459 As for precipitation representation, varres-CESM overestimates winter or annual precipitation
460 (about 40%-50%) especially along the western side of Sierra Nevada, and finer resolution simu-
461 lation produces a slight reduction (10%) likely due to improved treatment of orographic effects.
462 WRF 27km underestimates precipitation (about 30%) along the North coast and Sierra Nevada
463 mountains, where almost all the precipitation comes from, whereas WRF 9km shows a large
464 overestimation (about 70%–80%). Variability of precipitation ranges from 0 to 6 mm/day, with
465 generally higher inter-annual variability over locations of higher mean precipitation. For strong
466 precipitation events probability, varres-CESM and WRF 27km show satisfactory modeling ability
467 over most regions (except at the Central Valley for varres-CESM), although the reference datasets
468 also show some uncertainties.

469 Higher resolution (0.125°) simulation of varres-CESM do show better results in capturing sum-
470 mer Tmax, precipitation and their variability, than the coarser resolution run. However, the im-
471 provements are not statistically significant. For WRF, when resolution increased, the model pro-
472 duces obviously overestimated precipitation as previous studies have also found when using RCMs

473 for fine-scale simulations as aforementioned. The use convection scheme is perhaps not needed
474 when grid spacing is near 10km. However, it turned out that almost all of the precipitation comes
475 from resolved (large-scale) processes for all these models. In this way, model deviation is mainly
476 related with resolved-scale processes and microphysics scheme plays a major role, which makes
477 it necessary to develop more scale-aware parameterizations.

478 The importance and necessity of high resolution for regional climate studies has been widely
479 stressed by previous studies. However, whether the current regional climate models can fulfill this
480 demand when resolution is pushed to local scales is questionable. It is clear that further work is
481 urgently needed to solve the scale limitation of current regional climate models at fine horizontal
482 resolutions. The possible causes of the scale limitation may include a lack of accurate scale-aware
483 physical parameterizations near or below 10 km horizontal resolution, the treatment of dynamics
484 at fine scales, and the interactions among different components of RCMs or VR-GCMs (e.g., land-
485 atmosphere interactions).

486 In summary, varres-CESM demonstrated competitive utility for studying high-resolution re-
487 gional climatology when compared to a regional climate model (WRF) and a uniform high-
488 resolution GCM (CESM-FV). Deviations, showed within these models, are not indicative of deep
489 underlying problems with the model formulation, but one should be aware of these differences
490 when using these models for assessing future climate change. This study suggests that variable-
491 resolution GCMs are useful tools for assessing climate change over the coming century. As the
492 need for assessments of regional climate change is increasing, alternative modeling strategies, in-
493 cluding variable-resolution global climate models will be needed to improve our understanding of
494 the effects of fine-scale processes representation in regional climate regulation.

495 *Acknowledgments.* The authors would like to thank Michael Wehner and Daíthí Stone for pro-
496 viding the uniform resolution CESM dataset. We would further like to thank Travis O’Brien for
497 his many useful conversations on climate model assessment. We also want to thank Xuemeng
498 Chen for her assistance in WRF running. This project is supported in part by the University of
499 California, Davis and by the Department of Energy “Multiscale Methods for Accurate, Efficient,
500 and Scale-Aware Models of the Earth System” program.

501 **References**

- 502 Abatzoglou, J. T., K. T. Redmond, and L. M. Edwards, 2009: Classification of regional climate
503 variability in the state of California. *Journal of Applied Meteorology and Climatology*, **48** (8),
504 1527–1541.
- 505 Bacmeister, J. T., M. F. Wehner, R. B. Neale, A. Gettelman, C. Hannay, P. H. Lauritzen, J. M.
506 Caron, and J. E. Truesdale, 2014: Exploratory high-resolution climate simulations using the
507 Community Atmosphere Model (CAM). *Journal of Climate*, **27** (9), 3073–3099.
- 508 Bonfils, C., and D. Lobell, 2007: Empirical evidence for a recent slowdown in irrigation-induced
509 cooling. *Proceedings of the National Academy of Sciences*, **104** (34), 13 582–13 587.
- 510 Bukovsky, M. S., and D. J. Karoly, 2007: A brief evaluation of precipitation from the North
511 American Regional Reanalysis. *Journal of Hydrometeorology*, **8** (4), 837–846.
- 512 Bukovsky, M. S., and D. J. Karoly, 2009: Precipitation simulations using WRF as a nested regional
513 climate model. *Journal of Applied Meteorology and Climatology*, **48** (10), 2152–2159.
- 514 Caldwell, P., 2010: California wintertime precipitation bias in regional and global climate models.
515 *Journal of Applied Meteorology and Climatology*, **49** (10), 2147–2158.

- 516 Caldwell, P., H.-N. S. Chin, D. C. Bader, and G. Bala, 2009: Evaluation of a WRF dynamical
517 downscaling simulation over California. *Climatic Change*, **95** (3-4), 499–521.
- 518 Cayan, D. R., A. L. Luers, G. Franco, M. Hanemann, B. Croes, and E. Vine, 2008: Overview of
519 the California climate change scenarios project. *Climatic Change*, **87** (1), 1–6.
- 520 Chen, F., and J. Dudhia, 2001: Coupling an advanced land surface-hydrology model with the Penn
521 State-NCAR MM5 modeling system. Part I: Model implementation and sensitivity. *Monthly*
522 *Weather Review*, **129** (4), 569–585.
- 523 Chin, H.-N. S., P. M. Caldwell, and D. C. Bader, 2010: Preliminary study of California wintertime
524 model wet bias. *Monthly Weather Review*, **138** (9), 3556–3571.
- 525 Christensen, J. H., and Coauthors, 2007: Regional climate projections. *Climate Change, 2007: The Physical Science Basis. Contribution of Working group I to the Fourth Assessment Report of the Intergovernmental Panel on Climate Change, University Press, Cambridge, Chapter 11*,
526 847–940.
- 527
- 528 Collins, W. D., and Coauthors, 2004: Description of the NCAR community atmosphere model
529 (CAM 3.0). Tech. rep., Tech. Rep. NCAR/TN-464+ STR.
- 530
- 531 Daly, C., M. Halbleib, J. I. Smith, W. P. Gibson, M. K. Doggett, G. H. Taylor, J. Curtis, and P. P.
532 Pasteris, 2008: Physiographically sensitive mapping of climatological temperature and precip-
533 itation across the conterminous United States. *International Journal of Climatology*, **28** (15),
534 2031–2064.
- 535 Dee, D., and Coauthors, 2011: The ERA-Interim reanalysis: Configuration and performance of
536 the data assimilation system. *Quarterly Journal of the Royal Meteorological Society*, **137** (656),
537 553–597.

- 538 Dinse, K., 2009: Climate variability and climate change: what is the difference. *Book Climate*
539 *Variability and Climate Change: What is the Difference.*
- 540 Duffy, P., and Coauthors, 2006: Simulations of present and future climates in the western United
541 States with four nested regional climate models. *Journal of Climate*, **19** (6), 873–895.
- 542 Fox-Rabinovitz, M., J. Côté, B. Dugas, M. Déqué, and J. L. McGregor, 2006: Variable resolution
543 general circulation models: Stretched-grid model intercomparison project (SGMIP). *Journal of*
544 *Geophysical Research: Atmospheres (1984–2012)*, **111** (D16).
- 545 Fox-Rabinovitz, M. S., G. L. Stenchikov, M. J. Suarez, and L. L. Takacs, 1997: A finite-
546 difference GCM dynamical core with a variable-resolution stretched grid. *Monthly Weather*
547 *Review*, **125** (11), 2943–2968.
- 548 Fox-Rabinovitz, M. S., G. L. Stenchikov, M. J. Suarez, L. L. Takacs, and R. C. Govindaraju, 2000:
549 A uniform-and variable-resolution stretched-grid GCM dynamical core with realistic orography.
550 *Monthly Weather Review*, **128** (6), 1883–1898.
- 551 Fox-Rabinovitz, M. S., L. L. Takacs, R. C. Govindaraju, and M. J. Suarez, 2001: A variable-
552 resolution stretched-grid general circulation model: Regional climate simulation. *Monthly*
553 *Weather Review*, **129** (3), 453–469.
- 554 Gallus Jr, W. A., and J. F. Bresch, 2006: Comparison of impacts of WRF dynamic core, physics
555 package, and initial conditions on warm season rainfall forecasts. *Monthly Weather Review*,
556 **134** (9), 2632–2641.
- 557 Gates, W. L., 1992: AMIP: The Atmospheric Model Intercomparison Project. *Bulletin of the*
558 *American Meteorological Society*, **73**, 1962–1970.

- 559 Hamlet, A. F., and D. P. Lettenmaier, 2005: Production of Temporally Consistent Gridded Precipi-
560 tation and Temperature Fields for the Continental United States*. *Journal of Hydrometeorology*,
561 **6** (3), 330–336.
- 562 Hayhoe, K., and Coauthors, 2004: Emissions pathways, climate change, and impacts on Califor-
563 nia. *Proceedings of the National Academy of Sciences of the United States of America*, **101** (34),
564 12 422–12 427.
- 565 Hong, S.-Y., and J.-O. J. Lim, 2006: The WRF single-moment 6-class microphysics scheme
566 (WSM6). *Asia-Pacific Journal of Atmospheric Sciences*, **42** (2), 129–151.
- 567 Hong, S.-Y., Y. Noh, and J. Dudhia, 2006: A new vertical diffusion package with an explicit
568 treatment of entrainment processes. *Monthly Weather Review*, **134** (9), 2318–2341.
- 569 Hurrell, J. W., J. J. Hack, D. Shea, J. M. Caron, and J. Rosinski, 2008: A new sea surface temper-
570 ature and sea ice boundary dataset for the Community Atmosphere Model. *Journal of Climate*,
571 **21** (19), 5145–5153.
- 572 Hurrell, J. W., and Coauthors, 2013: The community earth system model: A framework for col-
573 laborative research. *Bulletin of the American Meteorological Society*, **94** (9), 1339–1360.
- 574 Jankov, I., W. A. Gallus Jr, M. Segal, B. Shaw, and S. E. Koch, 2005: The impact of different WRF
575 model physical parameterizations and their interactions on warm season MCS rainfall. *Weather
576 and Forecasting*, **20** (6), 1048–1060.
- 577 Kain, J. S., 2004: The Kain-Fritsch convective parameterization: An update. *Journal of Applied
578 Meteorology*, **43** (1), 170–181.

- 579 Kanamitsu, M., and H. Kanamaru, 2007: Fifty-seven-year California Reanalysis Downscaling at
580 10 km (CaRD10). Part I: System detail and validation with observations. *Journal of Climate*,
581 **20 (22)**, 5553–5571.
- 582 Kueppers, L. M., M. A. Snyder, and L. C. Sloan, 2007: Irrigation cooling effect: Regional climate
583 forcing by land-use change. *Geophysical Research Letters*, **34 (3)**.
- 584 Laprise, R., 2008: Regional climate modelling. *Journal of Computational Physics*, **227 (7)**, 3641–
585 3666.
- 586 Laprise, R., and Coauthors, 2008: Challenging some tenets of regional climate modelling. *Meteo-*
587 *rology and Atmospheric Physics*, **100 (1-4)**, 3–22.
- 588 Leung, L. R., L. O. Mearns, F. Giorgi, and R. L. Wilby, 2003a: Regional climate research: needs
589 and opportunities. *Bulletin of the American Meteorological Society*, **84 (1)**, 89–95.
- 590 Leung, L. R., and Y. Qian, 2009: Atmospheric rivers induced heavy precipitation and flooding in
591 the western US simulated by the WRF regional climate model. *Geophysical research letters*,
592 **36 (3)**.
- 593 Leung, L. R., Y. Qian, and X. Bian, 2003b: Hydroclimate of the western United States based on
594 observations and regional climate simulation of 1981-2000. Part I: Seasonal statistics. *Journal*
595 *of Climate*, **16 (12)**, 1892–1911.
- 596 Leung, L. R., Y. Qian, X. Bian, W. M. Washington, J. Han, and J. O. Roads, 2004: Mid-century
597 ensemble regional climate change scenarios for the western United States. *Climatic Change*,
598 **62 (1-3)**, 75–113.

- 599 Lo, J. C.-F., Z.-L. Yang, and R. A. Pielke, 2008: Assessment of three dynamical climate downscal-
600 ing methods using the Weather Research and Forecasting (WRF) model. *Journal of Geophysical*
601 *Research: Atmospheres (1984–2012)*, **113 (D9)**.
- 602 Maurer, E., A. Wood, J. Adam, D. Lettenmaier, and B. Nijssen, 2002: A long-term hydrologically
603 based dataset of land surface fluxes and states for the conterminous United States*. *Journal of*
604 *climate*, **15 (22)**, 3237–3251.
- 605 McDonald, A., 2003: Transparent boundary conditions for the shallow-water equations: testing in
606 a nested environment. *Monthly Weather Review*, **131 (4)**, 698–705.
- 607 Mearns, L. O., and Coauthors, 2012: The North American regional climate change assessment
608 program: overview of phase I results. *Bulletin of the American Meteorological Society*, **93 (9)**,
609 1337–1362.
- 610 Mesinger, F., and K. Veljovic, 2013: Limited area NWP and regional climate modeling: a test
611 of the relaxation vs Eta lateral boundary conditions. *Meteorology and Atmospheric Physics*,
612 **119 (1-2)**, 1–16.
- 613 Mesinger, F., and Coauthors, 2006: North American regional reanalysis. *Bulletin of the American*
614 *Meteorological Society*, **87**, 343–360.
- 615 Neale, R. B., and Coauthors, 2010a: Description of the NCAR community atmosphere model
616 (CAM 5.0). *NCAR Tech. Note NCAR/TN-486+STR*.
- 617 Neale, R. B., and Coauthors, 2010b: Description of the NCAR Community Atmosphere Model
618 (CAM 5.0). NCAR Technical Note NCAR/TN-486+STR, National Center for Atmospheric Re-
619 search, Boulder, Colorado, 268 pp.

- 620 Oleson, K., and Coauthors, 2010: Technical description of version 4.0 of the Community Land
621 Model (CLM). NCAR Technical Note NCAR/TN-478+STR, National Center for Atmospheric
622 Research, Boulder, Colorado, 257 pp. doi:10.5065/D6FB50WZ.
- 623 Pan, L.-L., S.-H. Chen, D. Cayan, M.-Y. Lin, Q. Hart, M.-H. Zhang, Y. Liu, and J. Wang, 2011:
624 Influences of climate change on California and Nevada regions revealed by a high-resolution
625 dynamical downscaling study. *Climate Dynamics*, **37** (9-10), 2005–2020.
- 626 Pierce, D. W., and Coauthors, 2013: Probabilistic estimates of future changes in California temper-
627 ature and precipitation using statistical and dynamical downscaling. *Climate Dynamics*, **40** (3-
628 4), 839–856.
- 629 Rauscher, S. A., E. Coppola, C. Piani, and F. Giorgi, 2010: Resolution effects on regional climate
630 model simulations of seasonal precipitation over Europe. *Climate Dynamics*, **35** (4), 685–711.
- 631 Rauscher, S. A., T. D. Ringler, W. C. Skamarock, and A. A. Mirin, 2013: Exploring a Global
632 Multiresolution Modeling Approach Using Aquaplanet Simulations. *Journal of Climate*, **26** (8),
633 2432–2452.
- 634 Ringler, T., L. Ju, and M. Gunzburger, 2008: A multiresolution method for climate system model-
635 ing: application of spherical centroidal voronoi tessellations. *Ocean Dynamics*, **58** (5-6), 475–
636 498.
- 637 Rummukainen, M., 2010: State-of-the-art with Regional Climate Models. *Wiley Interdisciplinary
638 Reviews: Climate Change*, **1** (1), 82–96.
- 639 Skamarock, W., J. Klemp, J. Dudhia, D. Gill, and D. Barker, 2005: Coauthors, 2008: A Descrip-
640 tion of the Advanced Research WRF Version 3. NCAR Technical Note. Tech. rep., NCAR/TN–
641 475+ STR.

- 642 Skamarock, W. C., and J. B. Klemp, 2008: A time-split nonhydrostatic atmospheric model for
643 weather research and forecasting applications. *Journal of Computational Physics*, **227** (7),
644 3465–3485.
- 645 Skamarock, W. C., J. B. Klemp, M. G. Duda, L. D. Fowler, S.-H. Park, and T. D. Ringler, 2012: A
646 multiscale nonhydrostatic atmospheric model using centroidal voronoi tessellations and c-grid
647 staggering. *Monthly Weather Review*, **140** (9), 3090–3105.
- 648 Soares, P. M., R. M. Cardoso, P. M. Miranda, J. de Medeiros, M. Belo-Pereira, and F. Espírito-
649 Santo, 2012: WRF high resolution dynamical downscaling of ERA-Interim for Portugal. *Cli-
650 mate dynamics*, **39** (9-10), 2497–2522.
- 651 Solomon, S., 2007: *Climate change 2007—the physical science basis: Working group I contribution
652 to the fourth assessment report of the IPCC*, Vol. 4. Cambridge University Press.
- 653 Staniforth, A. N., and H. L. Mitchell, 1978: A variable-resolution finite-element technique for
654 regional forecasting with the primitive equations. *Monthly Weather Review*, **106** (4), 439–447.
- 655 Stauffer, D. R., and N. L. Seaman, 1990: Use of four-dimensional data assimilation in a limited-
656 area mesoscale model. Part I: Experiments with synoptic-scale data. *Monthly Weather Review*,
657 **118** (6), 1250–1277.
- 658 Taylor, M. A., and A. Fournier, 2010: A compatible and conservative spectral element method on
659 unstructured grids. *Journal of Computational Physics*, **229** (17), 5879–5895.
- 660 Thornton, P. E., H. Hasenauer, and M. A. White, 2000: Simultaneous estimation of daily solar ra-
661 diation and humidity from observed temperature and precipitation: an application over complex
662 terrain in Austria. *Agricultural and Forest Meteorology*, **104** (4), 255–271.

- 663 Thornton, P. E., and S. W. Running, 1999: An improved algorithm for estimating incident daily
664 solar radiation from measurements of temperature, humidity, and precipitation. *Agricultural and*
665 *Forest Meteorology*, **93** (4), 211–228.
- 666 Thornton, P. E., S. W. Running, and M. A. White, 1997: Generating surfaces of daily meteorolog-
667 ical variables over large regions of complex terrain. *Journal of Hydrology*, **190** (3), 214–251.
- 668 Ullrich, P. A., 2014: SQuadGen: Spherical Quadrilateral Grid Generator. Accessed: 2015-02-11,
669 <http://climate.ucdavis.edu/squadgen.php>.
- 670 Warner, T. T., R. A. Peterson, and R. E. Treadon, 1997: A tutorial on lateral boundary conditions
671 as a basic and potentially serious limitation to regional numerical weather prediction. *Bulletin*
672 *of the American Meteorological Society*, **78** (11), 2599–2617.
- 673 Wehner, M., Prabhat, K. Reed, D. Stone, W. D. Collins, J. Bacmeister, and A. Gettleman, 2014a:
674 Resolution dependence of future tropical cyclone projections of CAM5.1 in the US CLIVAR
675 Hurricane Working Group idealized configurations. *J. Climate*, doi:10.1175/JCLI-D-14-00311.
676 1, in press.
- 677 Wehner, M. F., and Coauthors, 2014b: The effect of horizontal resolution on simulation qual-
678 ity in the Community Atmospheric Model, CAM5.1. *J. Model. Earth. Sys.*, doi:10.1002/
679 2013MS000276.
- 680 Zarzycki, C. M., and C. Jablonowski, 2014: A multidecadal simulation of Atlantic tropical cy-
681 clones using a variable-resolution global atmospheric general circulation model. *Journal of Ad-*
682 *vances in Modeling Earth Systems*, **6** (3), 805–828.

683 Zarzycki, C. M., C. Jablonowski, and M. A. Taylor, 2014: Using Variable-Resolution Meshes
684 to Model Tropical Cyclones in the Community Atmosphere Model. *Monthly Weather Review*,
685 **142** (3), 1221–1239.

686 Zarzycki, C. M., C. Jablonowski, D. R. Thatcher, and M. A. Taylor, 2015: Effects of localized
687 grid refinement on the general circulation and climatology in the community atmosphere model.
688 *Journal of Climate*, **28** (7), 2777–2803.

689 **LIST OF TABLES**

TABLE 1. Reanalysis and statistically downscaled observational datasets used in this study.

Data source	Variables used	Spatial resolution	Temporal resolution
NARR	Pr, T_s	32km	daily, 3-hourly
NCEP CPC	Pr	0.25°	daily
UW	Pr, T_{min} , T_{max}	0.125°	daily
PRISM	Pr, T_{min} , T_{max} , T_{avg}	4km	monthly
Daymet	Pr, T_{min} , T_{max}	1km	daily

TABLE 2. RMSD, MAD and Correlation (Corr) for JJA temperature over California

RMSD	UW		PRISM			Daymet	
	T_{max}	T_{min}	T_{max}	T_{min}	T_{avg}	T_{max}	T_{min}
varres-CESM 0.25d	2.322	3.745	2.924	3.121	2.604	2.810	3.934
varres-CESM 0.125d	1.900	3.631	2.447	2.944	2.184	2.475	3.701
WRF 27km	2.310	2.738	2.933	2.254	2.169	2.511	2.992
WRF 9km	3.319	2.937	3.492	1.837	1.769	3.203	2.942
uniform CESM 0.25d	3.885	4.088	4.265	3.614	3.536	4.315	4.274

MAD	UW		PRISM			Daymet	
	T_{max}	T_{min}	T_{max}	T_{min}	T_{avg}	T_{max}	T_{min}
varres-CESM 0.25d	0.981	2.907	0.606	1.731	0.823	1.177	2.877
varres-CESM 0.125d	0.645	2.848	0.203	1.660	0.579	0.818	2.744
WRF 27km	-0.577	0.819	-0.952	-0.357	-0.771	-0.386	0.789
WRF 9km	-2.277	1.862	-2.720	0.674	-1.142	-2.103	1.757
uniform CESM 0.25d	1.812	2.993	1.449	1.815	1.280	2.013	2.961

Corr	UW		PRISM			Daymet	
	T_{max}	T_{min}	T_{max}	T_{min}	T_{avg}	T_{max}	T_{min}
varres-CESM 0.25d	0.998	0.982	0.996	0.986	0.994	0.997	0.979
varres-CESM 0.125d	0.998	0.985	0.997	0.988	0.996	0.997	0.983
WRF 27km	0.997	0.982	0.996	0.989	0.996	0.997	0.978
WRF 9km	0.996	0.985	0.997	0.993	0.998	0.996	0.984
uniform CESM 0.25d	0.994	0.980	0.992	0.981	0.991	0.993	0.977

690 TABLE 3. The first four moments of the JJA Tmax frequency in each sub-zone. Column titles refer to Average
 691 (Avg), Variance (Var), Skewness (Skew) and Kurtosis (Kurt).

	Central valley				Mountain				North coast				South coast				Desert			
	Avg	Var	Skew	Kurt	Avg	Var	Skew	Kurt	Avg	Var	Skew	Kurt	Avg	Var	Skew	Kurt	Avg	Var	Skew	Kurt
UW	32.6	24.8	-0.8	0.9	26.7	33.2	-0.4	0.3	25.9	30.4	0.1	-0.5	25.9	30.4	0.1	-0.5	37.0	22.9	-0.6	0.7
Daymet	32.7	23.5	-0.9	1.5	25.9	39.3	-0.5	0.5	26.5	30.1	-0.3	0.4	26.5	30.1	-0.3	0.4	37.0	24.3	-0.6	0.6
CESM 0.25d	34.1	26.2	-0.4	0.2	28.1	27.6	-0.4	0.3	26.4	37.4	0.1	-0.7	26.4	37.4	0.1	-0.7	37.6	19.0	-0.5	0.8
CESM 0.125d	34.3	28.5	-0.5	0.4	27.2	30.0	-0.4	0.3	26.3	37.4	0.1	-0.6	26.3	37.4	0.1	-0.6	37.3	21.3	-0.5	0.4
WRF 27km	33.9	34.8	-0.5	0.2	24.9	34.8	-0.3	0.0	26.0	36.7	-0.1	-0.5	26.0	36.7	-0.1	-0.5	36.5	22.6	-0.6	0.5
WRF 9km	32.4	33.1	-0.7	0.6	22.4	38.5	-0.5	0.6	24.9	32.6	0.0	-0.6	24.9	32.6	0.0	-0.6	34.4	24.4	-0.5	0.4

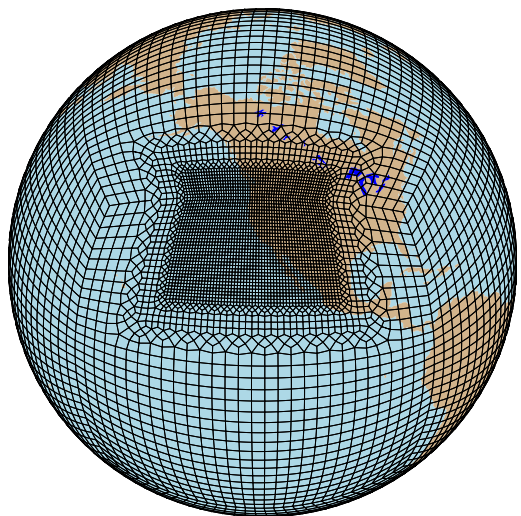
Notes: If skew > 0 [skew < 0], the distribution trails off to the right [left]. If kurtosis > 0 [< 0], it is usually more sharply peaked [flatter] than the normal distribution (leptokurtic and platykurtic, respectively).

TABLE 4. RMSD, MAD, MRD, Correlation (Corr) for precipitation over California

Annual	CPC				UW				PRISM				DAYMET				
	RMSD	MAD	MRD	Corr	RMSD	MAD	MRD	Corr	RMSD	MAD	MRD	Corr	RMSD	MAD	MRD	Corr	
varres-CESM 0.25d	0.607	0.394	0.413	0.981	0.616	0.292	0.434	0.968	0.727	0.203	0.429	0.952	0.567	0.191	0.375	0.972	
varres-CESM 0.125d	0.469	0.207	0.321	0.980	0.526	0.115	0.339	0.970	0.624	0.045	0.328	0.961	0.504	0.027	0.310	0.973	
WRF 27km	0.419	-0.205	0.269	0.977	0.580	-0.308	0.274	0.971	0.765	-0.396	0.296	0.965	0.647	-0.409	0.312	0.970	
WRF 9km	2.226	1.485	0.950	0.957	2.052	1.393	0.864	0.964	1.889	1.322	0.815	0.970	2.005	1.306	0.773	0.961	
uniform CESM 0.25d	0.555	0.134	0.277	0.969	0.600	0.031	0.302	0.961	0.700	-0.057	0.290	0.953	0.600	-0.069	0.284	0.962	
DJF		CPC				UW				PRISM				DAYMET			
		RMSD	MAD	MRD	Corr	RMSD	MAD	MRD	Corr	RMSD	MAD	MRD	Corr	RMSD	MAD	MRD	Corr
varres-CESM 0.25d	1.486	0.986	0.532	0.972	1.445	0.673	0.531	0.959	1.654	0.577	0.547	0.943	1.346	0.514	0.435	0.964	
varres-CESM 0.125d	1.194	0.638	0.396	0.976	1.234	0.346	0.398	0.965	1.395	0.287	0.400	0.955	1.170	0.212	0.337	0.969	
WRF 27km	0.888	-0.376	0.269	0.975	1.289	-0.688	0.289	0.967	1.552	-0.785	0.298	0.962	1.351	-0.848	0.324	0.966	
WRF 9km	4.264	2.607	0.742	0.950	3.835	2.315	0.616	0.955	3.570	2.256	0.604	0.964	3.804	2.183	0.554	0.955	
uniform CESM 0.25d	1.392	0.377	0.300	0.960	1.431	0.064	0.316	0.951	1.544	-0.033	0.314	0.946	1.406	-0.095	0.288	0.953	

692 **LIST OF FIGURES**

1 degree -> 0.25 degree



1 degree -> 0.125 degree

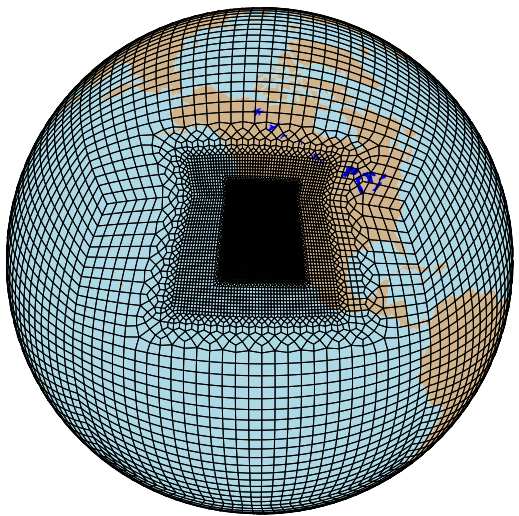
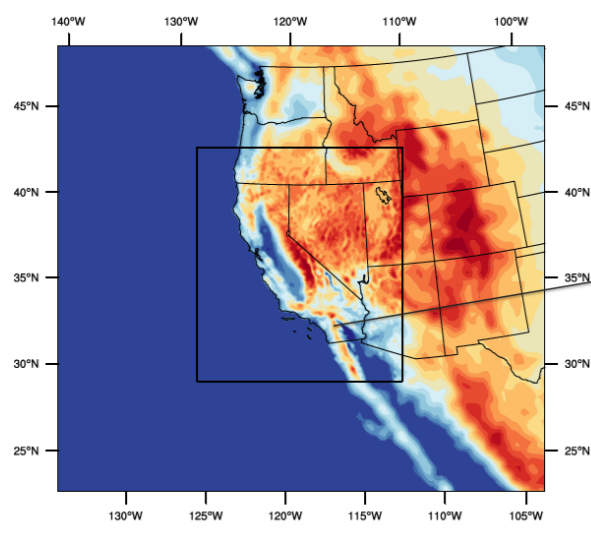
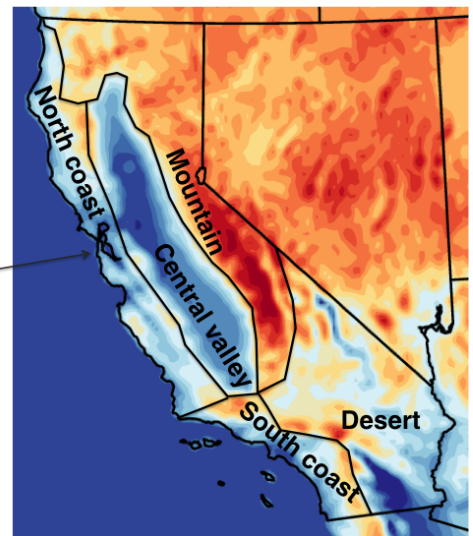


FIG. 1. Grid meshes for the two varres-CESM simulations.

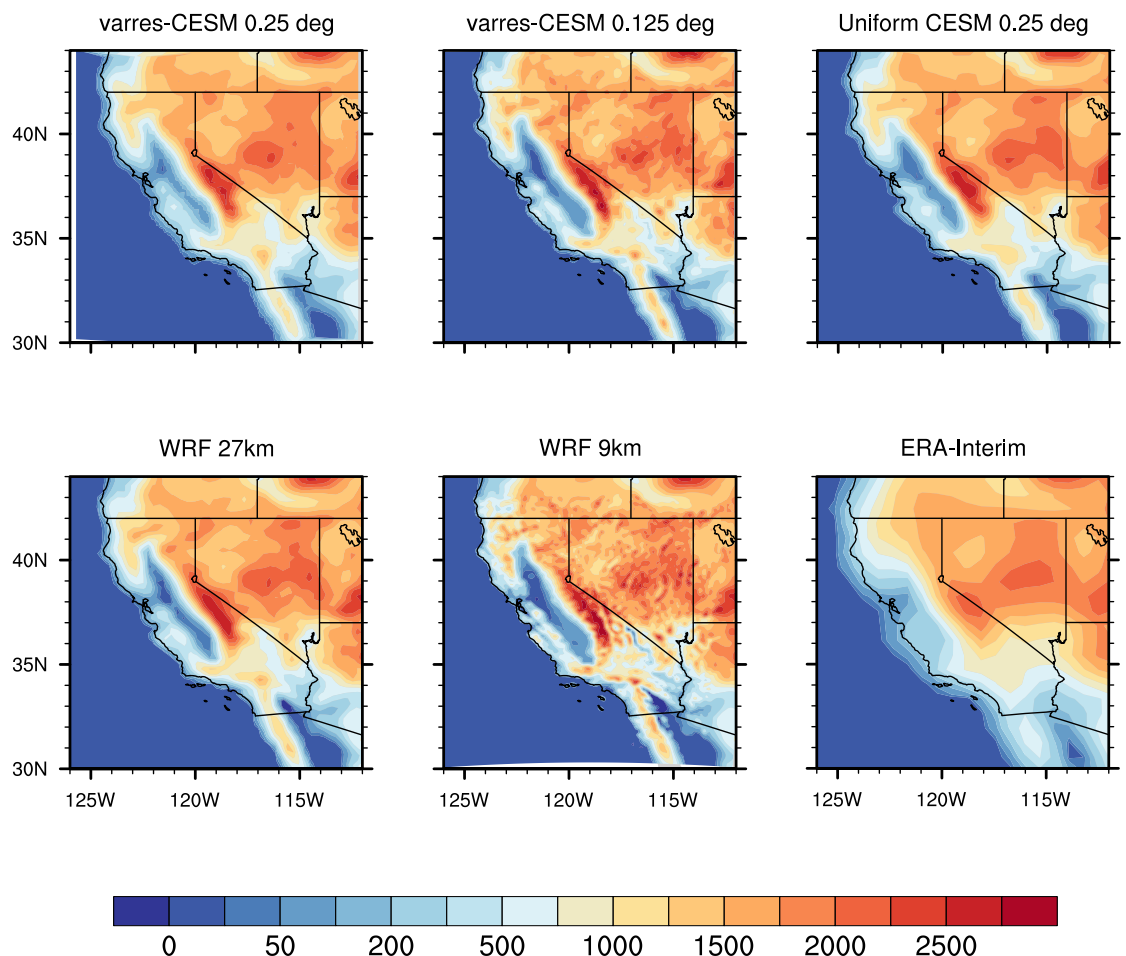
WRF 9km : Outer and inner domain



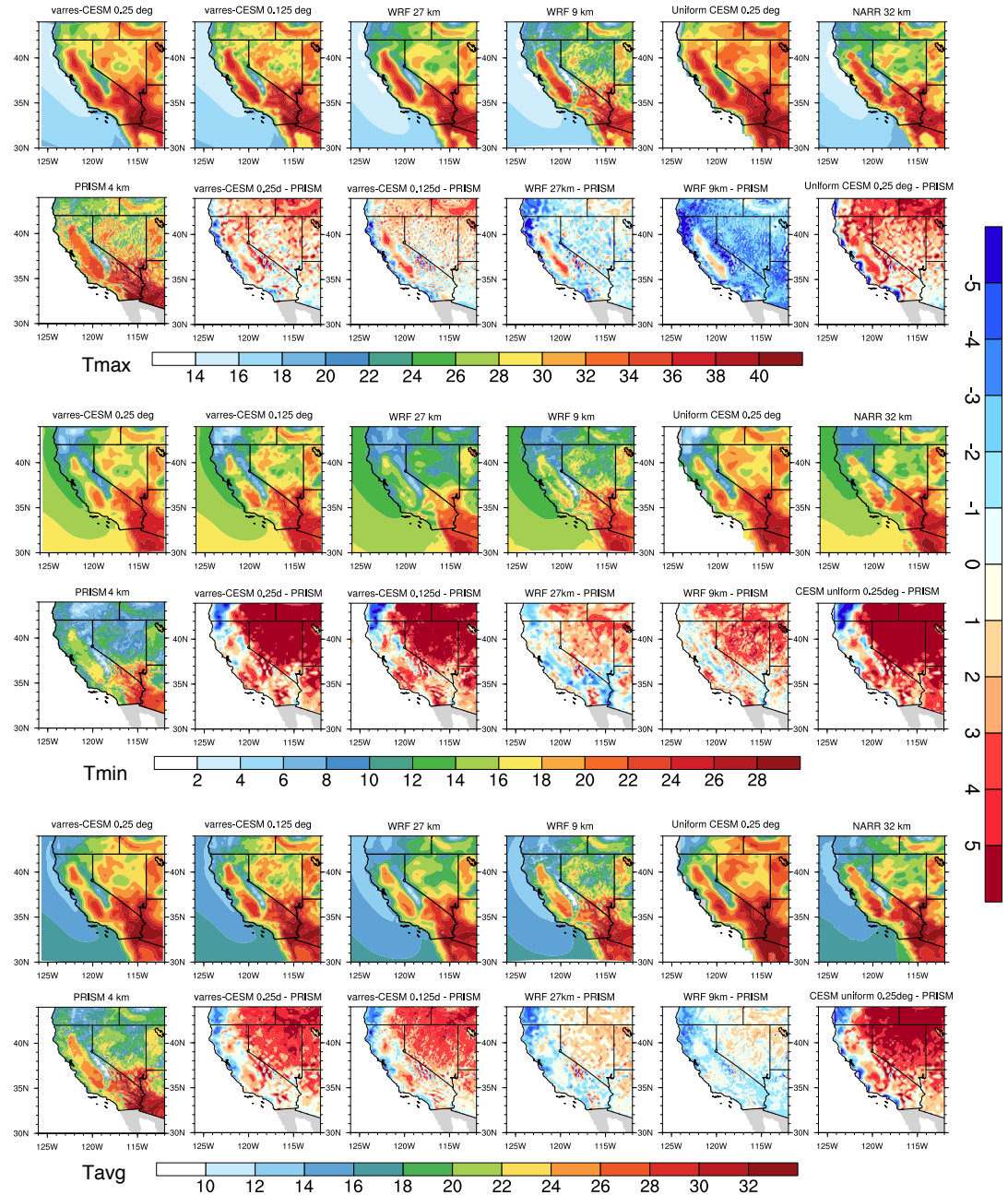
Climate divisions across CA



693 FIG. 2. Domains of WRF simulations (left) and five climate divisions in California (right) with topography in
694 meters (m).



695 FIG. 3. Topography in meters (m) for (top left to bottom right) varres-CESM 0.25° , varres-CESM 0.125° ,
696 uniform CESM-FV 0.25° , WRF 27km, WRF 9km and ERA-Interim (~ 80 km).



697 FIG. 4. JJA average daily Tmax, Tmin and Tavg from models and reference datasets, and differences between
 698 models and PRISM ($^{\circ}\text{C}$).

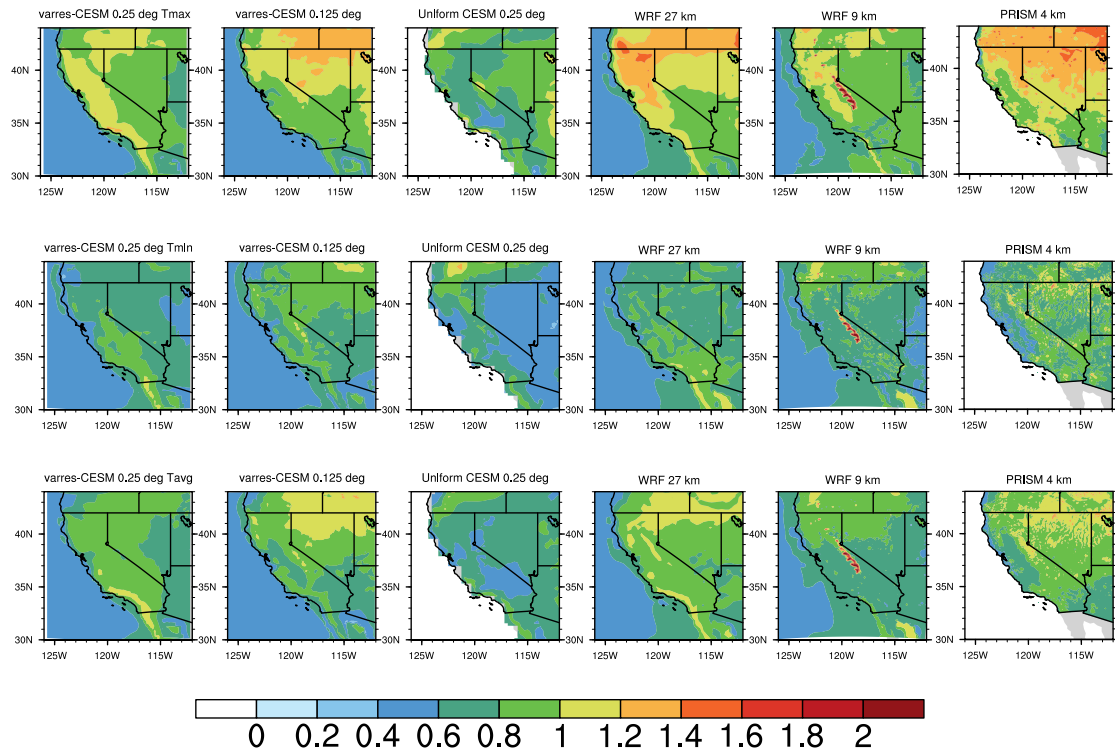


FIG. 5. sample standard deviation of JJA average daily Tmax, Tmin and Tavg from models and PRISM ($^{\circ}\text{C}$).

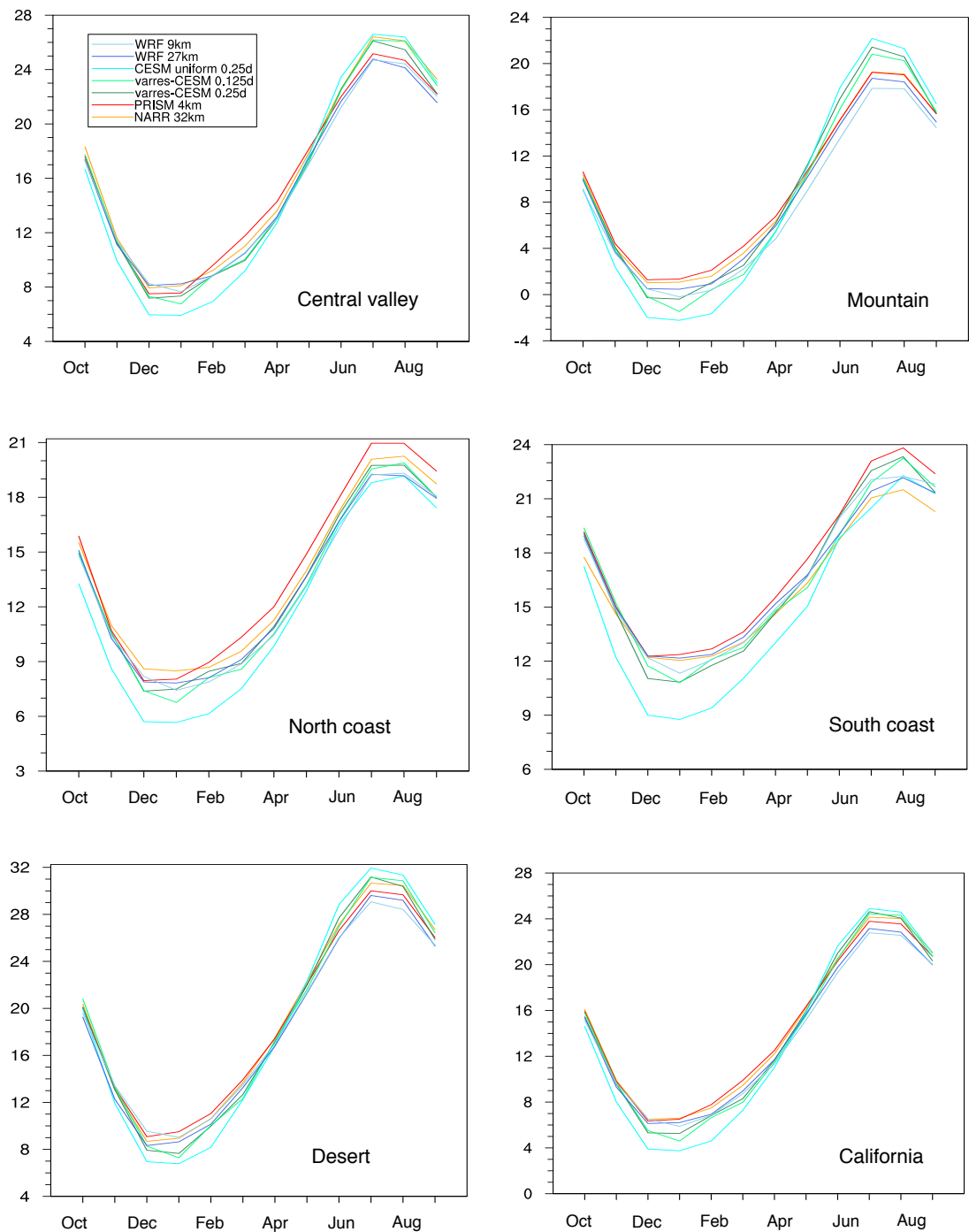


FIG. 6. Seasonal cycle of monthly-average Tavg for each subzone ($^{\circ}\text{C}$).

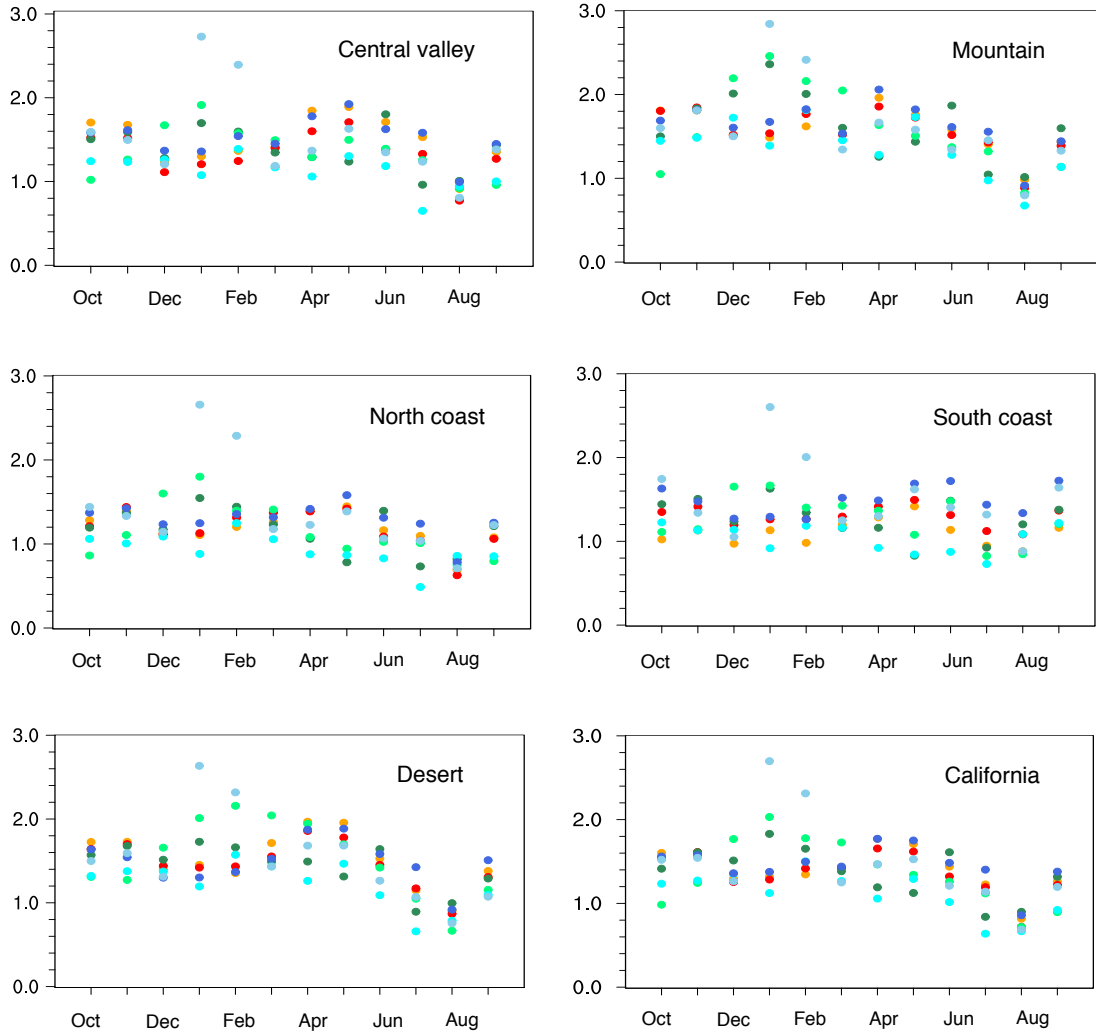


FIG. 7. Seasonal standard deviation (s) values of monthly-average T_{avg} for each subzone ($^{\circ}C$).

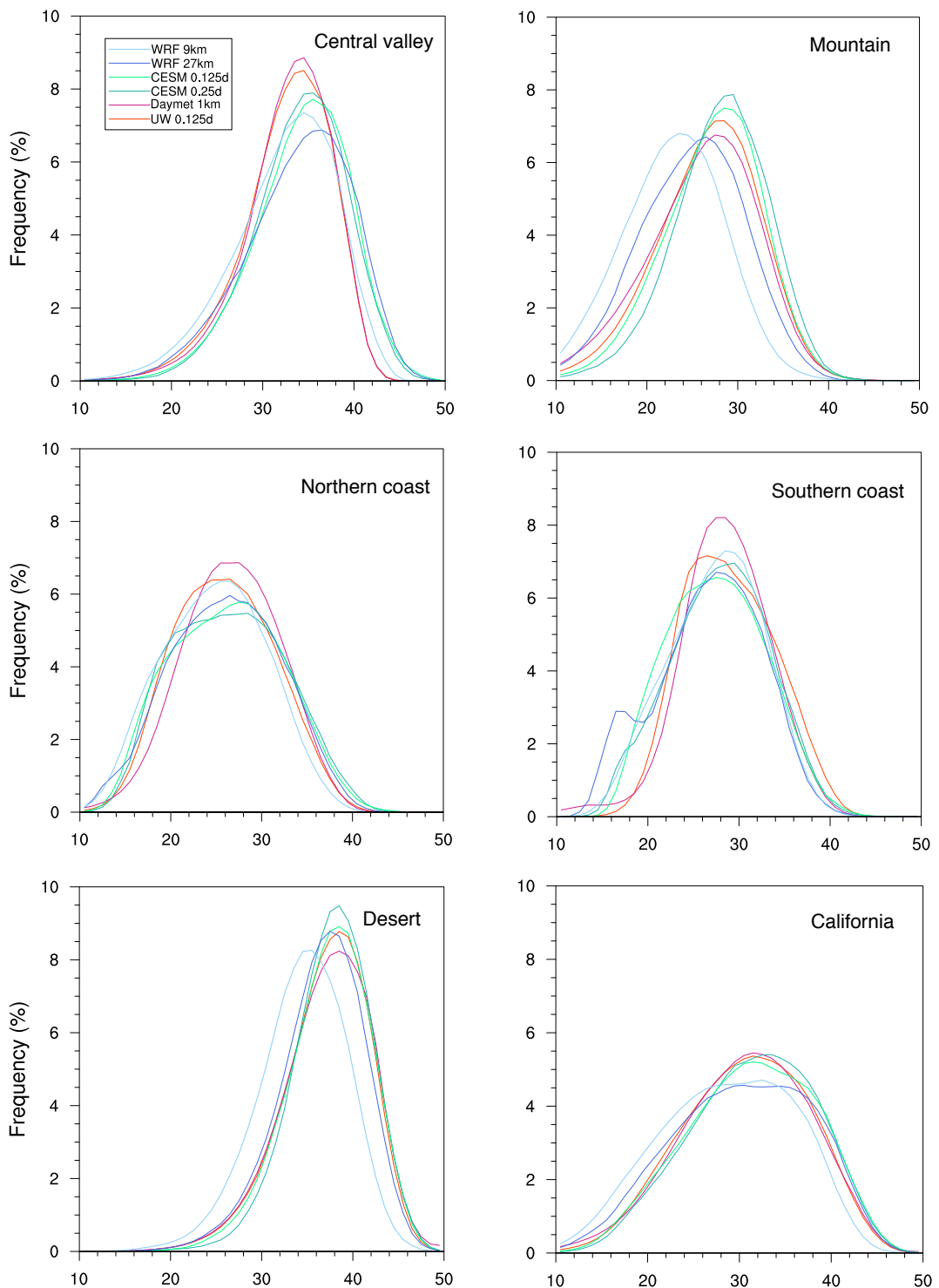
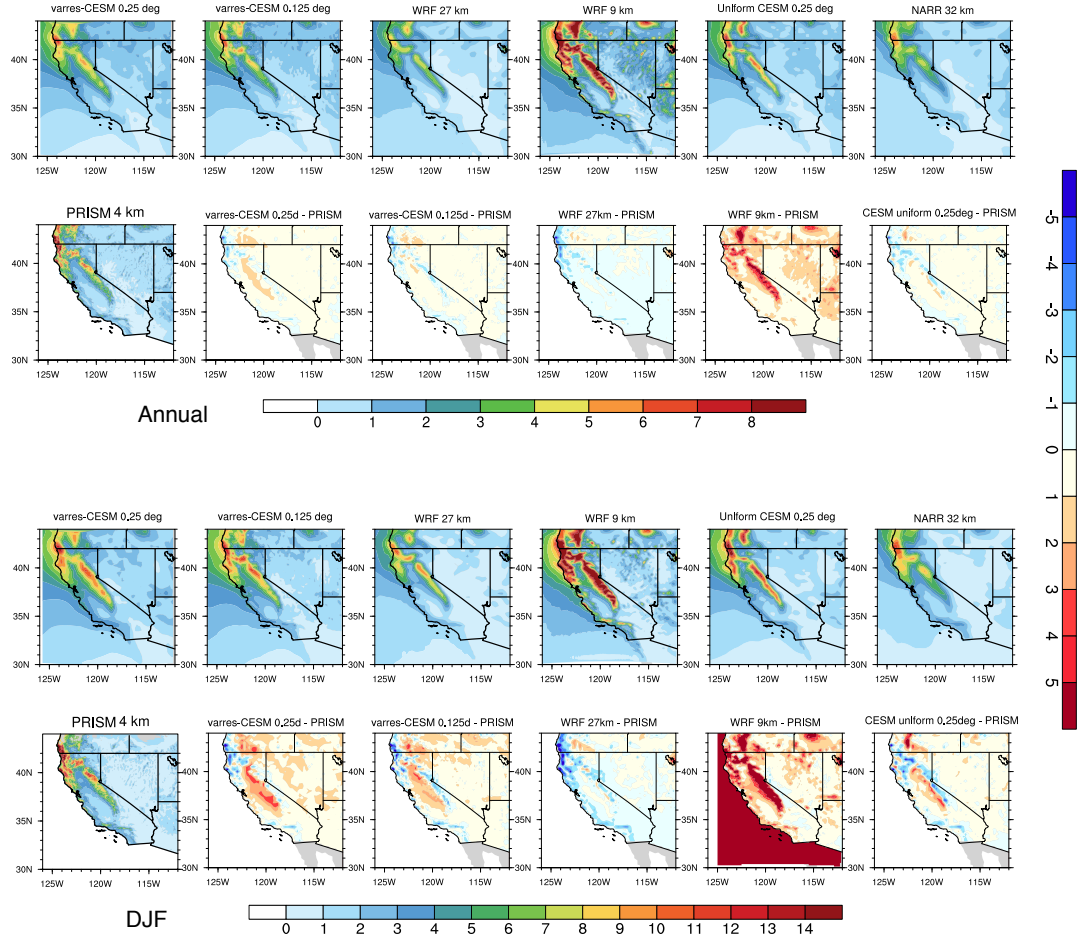


FIG. 8. Frequency distribution of summer Tmax ($^{\circ}\text{C}$).



699 FIG. 9. Annual and DJF precipitation from models and reference datasets, and differences between models
 700 and PRISM (mm/d).

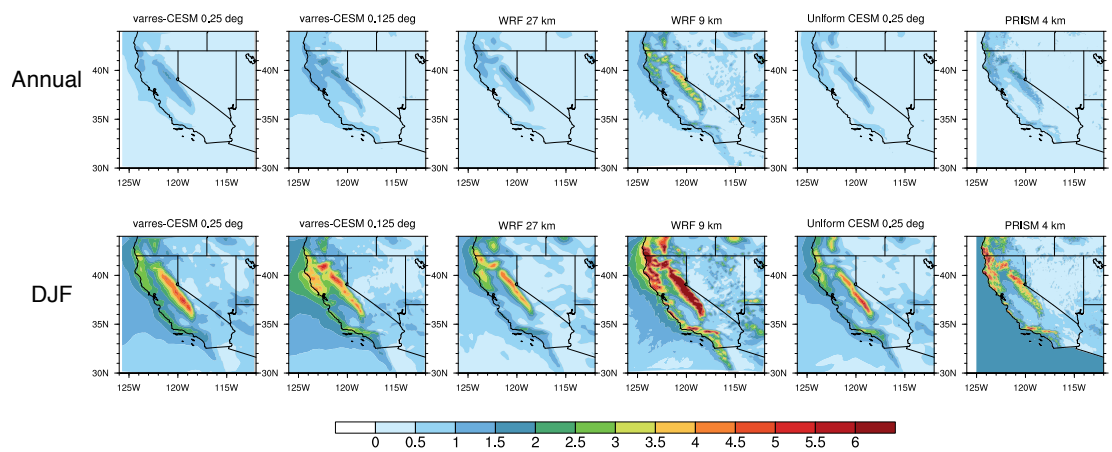


FIG. 10. sample standard deviation of Annual and DJF precipitation from models and PRISM (mm/d).

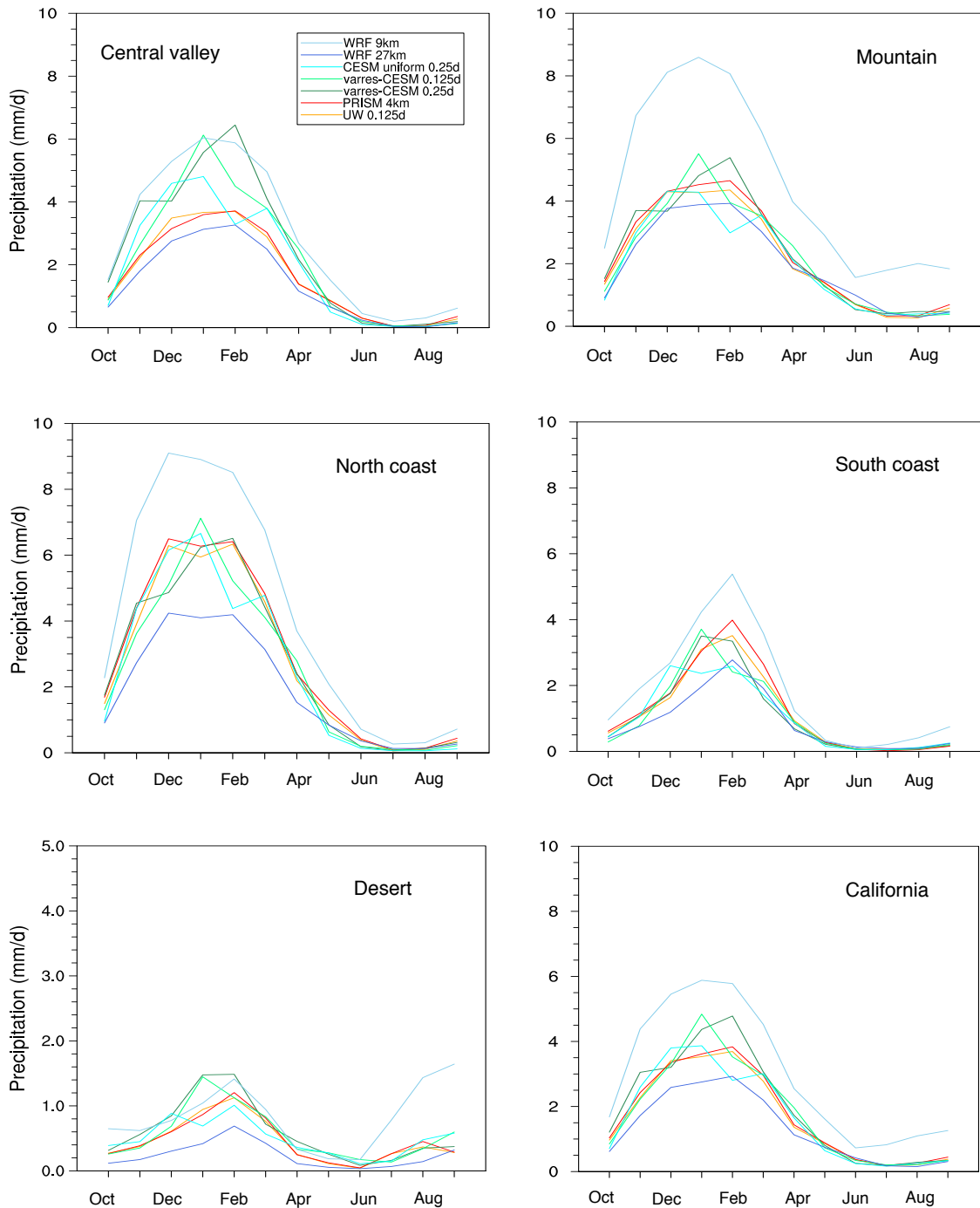


FIG. 11. As Figure 6, but for monthly-average total precipitation (mm/d).

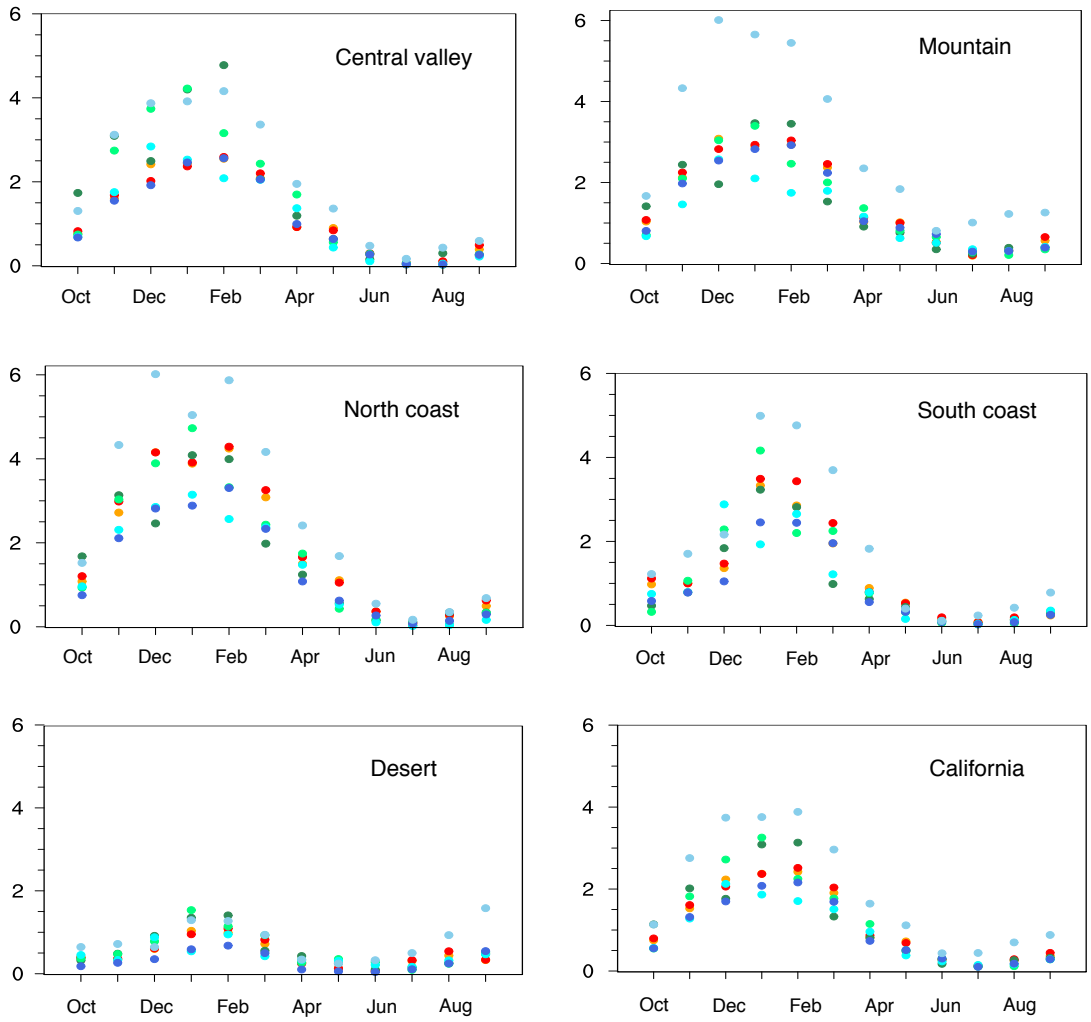
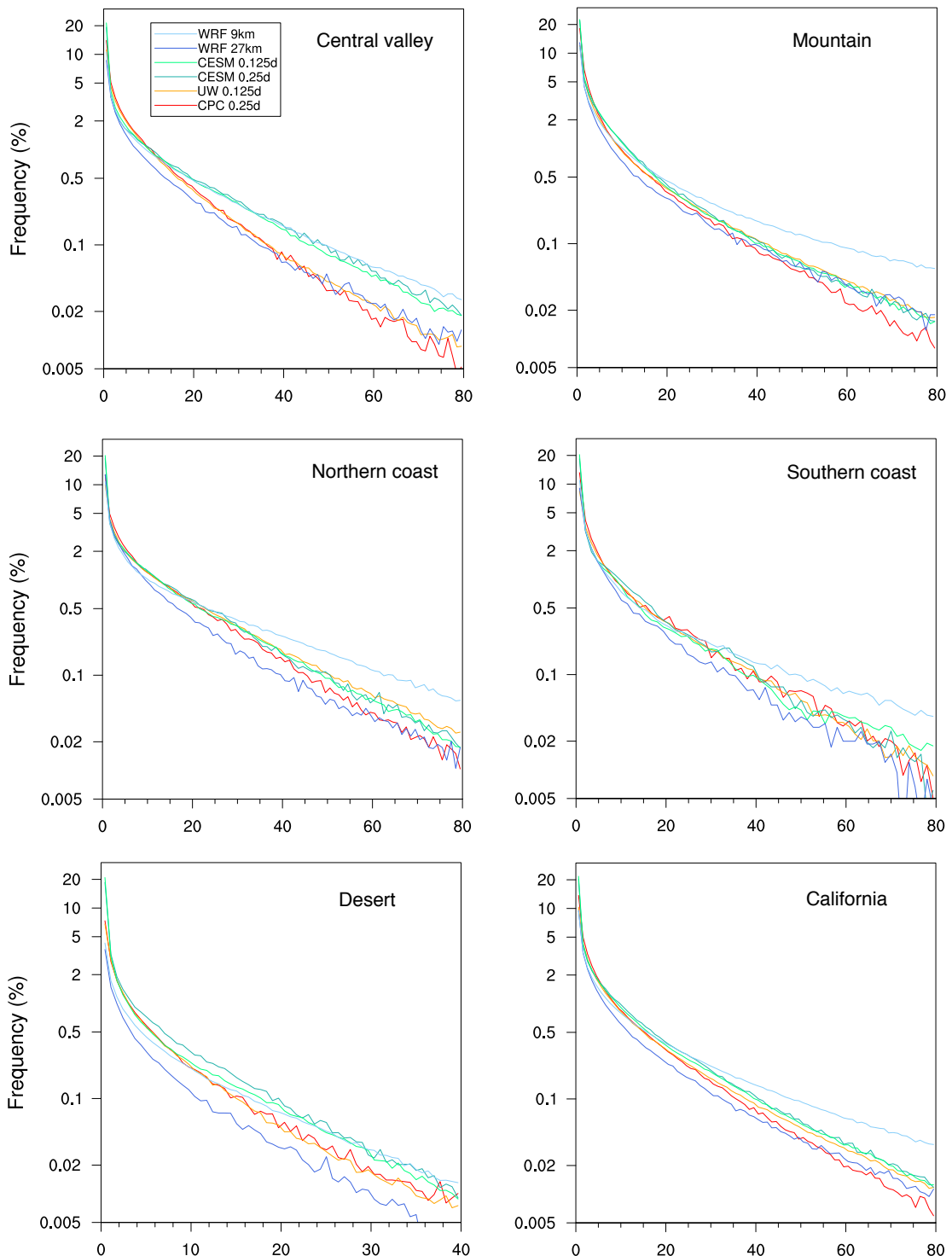
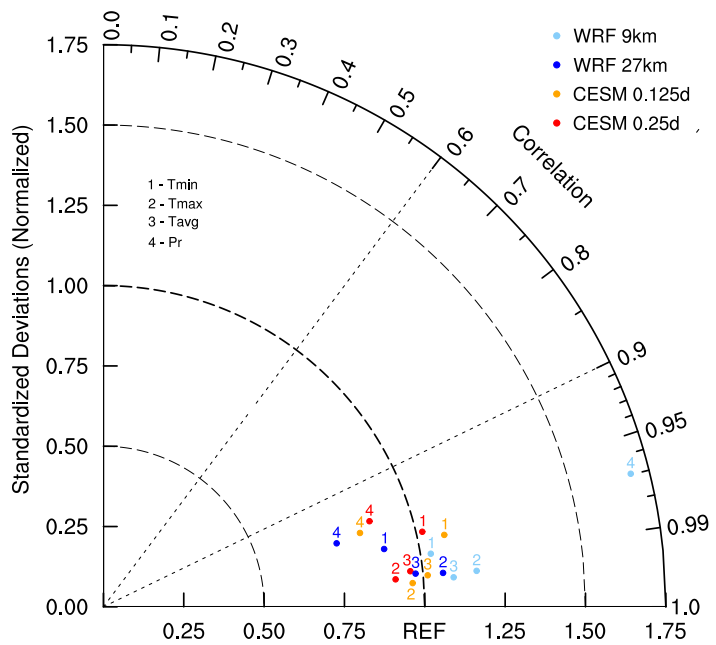


FIG. 12. As Figure 7, but for monthly-average total precipitation (mm/d).



701 FIG. 13. Frequency distribution of winter Pr, the unit of x-axis is mm/d (note that the vertical scale is loga-
 702 rithmic).



703 FIG. 14. Taylor diagram of annual climatology for the entire California region, using the PRISM dataset as
 704 reference.